

**Lacustrine sedimentation in active volcanic settings:
The Late Quaternary depositional evolution of Lake Chungará (Northern Chile)**

Sáez, A.^{1*}, Valero-Garcés, B.L.², Moreno, A.², Bao, R.³, Pueyo, J.J.¹, González-Sampériz, P.²,
Giralt, S.⁴, Taberner, C.⁴, Herrera, C.⁵, and Gibert, R.O.¹

¹ Facultat de Geologia, Universitat de Barcelona, c/ Martí Franques s/n, 08028 Barcelona (Spain)

² Instituto Pirenaico de Ecología. Consejo Superior de Investigaciones Científicas. Apdo 202, 50080 Zaragoza (Spain)

³ Facultade de Ciencias, Universidade da Coruña, Campus da Zapateira s/n, 15071 A Coruña (Spain)

⁴ Instituto de Ciencias de la Tierra 'Jaume Almera' - CSIC, c/ Lluís Sole Sabaris s/n, 08028 Barcelona (Spain)

⁵ Departamento de Ciencias Geológicas, Universidad Católica del Norte, Casilla 1280, Antofagasta (Chile)

(*) E-mail: a.saez@ub.edu

ABSTRACT

Lake Chungará is the largest (22.5 Km²) and deepest (40 m) lacustrine ecosystem in the Chilean Altiplano and its location in an active volcanic setting provides an opportunity to evaluate environmental (volcanic versus climatic) controls on lacustrine sedimentation. The Late Quaternary depositional history of Lake Chungará (18°15' S, 69°09' W, 4520 m a.s.l.) is reconstructed by means of a multiproxy study of 15 Kullenberg cores and seismic data. The chronological framework is supported by 10 ¹⁴C AMS and 1 ²³⁰Th/²³⁴U dates. Lake Chungará was formed prior to 12.8 cal. kyr BP following the partial collapse of the Parinacota volcano that impounded the Lauca river. The sedimentary architecture of the lacustrine sequence has been controlled by (1) the strong inherited palaeo-relief, and (2) changes in the accommodation, caused by lake level fluctuations and tectonic subsidence. The first factor determined the location of the depocentre in the NW of the central plain. The second factor caused the area of deposition to extend towards the eastern and southern basin margins with accumulation of high-stand sediments on the elevated marginal platforms. Synsedimentary normal faulting also increased accommodation and increased the rate of sedimentation rate in the northern part of the basin. Six sedimentary units were identified and correlated in the basin mainly using tephra keybeds. Unit 1 (Late Pleistocene - early Holocene) is made up of laminated diatomite with some carbonate-rich (calcite and aragonite) laminae. Unit 2 (mid Holocene - Recent) is composed of massive to bedded diatomite with abundant tephra (lapilli and ash) layers. Some carbonate-rich layers (calcite and aragonite) occur. Unit 3 consists of macrophyte-rich diatomite deposited in nearshore environments. Unit 4 is composed of littoral sediments dominated by alternating charophyte-rich and other aquatic macrophyte-rich facies. Littoral carbonate productivity peaked when suitable shallow platforms were available for charophyte colonization. Clastic deposits in the lake are restricted to lake margins (Units 5 and 6). Diatom productivity peaked during a lowstand period (Unit 1 and Subunit 2a), and was probably favoured by photic conditions affecting larger areas of the lake bottom. Offshore carbonate precipitation reached its maximum during the early to mid Holocene (c. 7.8 and 6.4 cal. kyr BP). This may have been favoured by increases in lake solute concentrations resulting from evaporation and calcium input due to the compositional changes in pyroclastic supply. Diatom and pollen data from offshore cores suggest a number of lake level fluctuations: a Late Pleistocene deepening episode (c. 12.6 cal kyr BP), four shallowing episodes during the early to mid Holocene (c. 10.5, 9.8, 7.8 and 6.7 cal. kyr BP) and higher lake levels since the mid Holocene (c. 5.7 cal kyr BP) till the present. Explosive activity at Parinacota volcano was very limited between c. >12.8 and 7.8 cal kyr BP. Mafic-rich explosive eruptions from the Ajata satellite cones increased after c. 5.7 cal kyr BP till the present.

Keywords: Andean Altiplano, Holocene, diatomite, tephra, carbonate, lacustrine ecosystem

INTRODUCTION

Sedimentary successions of lakes in active volcanic areas in the Andean Altiplano have provided detailed records of global changes (environmental, climatic and cultural) during the Late Quaternary (Grosjean, 1994, Grosjean *et al.*, 1997, 2001; Valero-Garcés *et al.*, 1999b). Many of the palaeoenvironmental and palaeohydrological fluctuations have

been attributed to climatic variability. However, given the active volcanism and related tectonics in the region, the role of volcanic processes in lacustrine sedimentation requires evaluation. Volcanic activity may strongly influence lake deposition by several processes: i) changes in the vegetation of the lake catchments due to increased wildfires and variations in soil conditions favourable to pioneer plants (Haberle *et al.*, 2000); ii) changes in bathymetry and morphology of the lake basin caused by faulting and the construction and erosion of volcanic structures (Colman *et al.* 2002); iii) variability in the sediment supply to the lake and in the chemistry of the waters due to the supply of new volcanic materials in the watershed and to the direct input of pyroclastic material into the lake (Telford *et al.* 2004); iv) addition of hydrothermal fluids to the lake system changing the chemistry of water and sediments (Valero-Garcés *et al.*, 1999a); and v) ecological impacts on the aquatic ecosystems (Baker, *et al.* 2003).

Lake Chungará (18°15' S, 69°09' W, 4520 m a.s.l.), at the base of the active Parinacota volcano (6342 m a.s.l.), is the deepest and highest lacustrine ecosystem in the Chilean Altiplano. The sedimentary record, including diatomite-dominated sediments and tephra layers, provides a unique opportunity to analyze the interplay of climate change (Grosjean, 1994, Grosjean *et al.*, 1997, 2001, Valero-Garcés, 1999) and the activity of the Parinacota volcano during the Holocene (Wörner *et al.*, 1988, 2000; Clavero *et al.*, 2002, 2004).

A seismic survey and some littoral cores obtained in 1993 provided a preliminary reconstruction of the Late Quaternary evolution of the lake (Valero-Garcés *et al.*, 1999b, 2000, 2003). In November 2002, a coring expedition with the Limnological Research Center (University of Minnesota, USA) retrieved 15 Kullenberg cores up to 8 m long along several transects in the lake basin. Stratigraphical and sedimentological analyses of the new cores and integration with the seismic profiles allowed the 3D reconstruction of the lake sediment architecture. The chronological framework was based on ^{14}C AMS and $^{230}\text{Th}/^{234}\text{U}$ methods. The interpreted depositional environments may serve as modern analogues of lacustrine sedimentation Quaternary and pre-Quaternary volcanic settings elsewhere. Diatomaceous sediments occur in a variety of Quaternary and pre-Quaternary lake succession (Bellanca *et al.* 1989; Owen & Crossley, 1992; Owen & Utha-aroon, 1999; Zheng & Lei, 1999; Sáez *et al.*, 1999), often in volcanic-influenced basins where volcanic silica and hot waters provide the dissolved silica necessary for diatom growth. The variety of diatomite facies from Lake Chungará illustrates the large compositional range of diatomite in a single basin. Diatomite commonly occurs with other offshore and littoral facies such as alluvial, carbonate-rich (Gasse *et al.*, 1987; Bao *et al.*, 1999) and aquatic macrophyte-rich facies. A multiproxy approach enabled us to characterize the roles of tectonics, volcanism and climate change in lake evolution.

GEOLOGICAL SETTING

The Lauca Basin and the origin of Lake Chungará

Lake Chungará is located on the northeastern edge of the Lauca Basin (Fig. 1), an intra-arc basin bounded by faults and volcanoes. The peaks of the Western Andean Cordillera (up to 5000 m a.s.l.) form the western margin, and a N-S ridge made up of Parinacota, Quisquisini, Guallatire and Puquintica volcanoes forms the eastern margin (Fig. 1A). The Lauca Basin is filled with an Upper Miocene to Pliocene volcanoclastic, alluvial and lacustrine sedimentary succession, >120 m thick, of that rests unconformably on an Upper Cretaceous - Lower Miocene volcanic substrate (Kött *et al.*, 1995; Gaupp *et al.*, 1999). During the Late Pleistocene, the Palaeo-Lauca River flowed northward from Guallatire to Cotacotani, between Ajoya and Parinacota volcanoes, turned westward at Parinacota, then flowed southwards for about 100 km, and finally eastwards to Bolivia. Lacustrine depositional environments also occurred during the Late Pleistocene in the northern areas close to the village of Parinacota (Fig. 1A).

Parinacota volcano (6342 m a.s.l.) is a large composite stratocone of Late Quaternary age. It is built on an earlier stratocone in the Lauca Basin that underwent a single catastrophic sector collapse event and produced a c. 6 km³ debris-avalanche deposit that covered more than 140 km² (Francis & Wells, 1988; Wörner *et al.*, 1988, 2000; Clavero *et al.*, 2002, 2004). The debris avalanche buried fluvial and lacustrine formations, dammed the Palaeo-Lauca River and isolated the Chungará Subbasin (273 km²) to the south, which became topographically-closed without any surface outlets (Fig. 1A). The pronounced hummock topography of the avalanche deposit also created new lakes within the Parinacota debris (the present-day Cotacotani lakes, Fig. 1). At the lowest topographic level of both subbasins, lakes formed almost immediately: the Cotacotani lakes and Lake Chungará (Fig. 1B). A minimum age for the collapse, between 11,155 and 13,500 ^{14}C yr BP, was obtained by ^{14}C dating the post-avalanche Cotacotani lake sediments (Francis & Wells, 1988; Ammann *et al.*, 2001, Baied & Wheeler, 1993) and 18,000 cal yr BP using He-exposure techniques (Wörner *et al.*, 2000). Clavero *et al.* (2002, 2004) dated palaeosoil horizons and suggested a maximum age of 8000 ^{14}C yr BP for the collapse. The differences reflect the different interpretations of the stratigraphic location of the analyzed samples: Clavero *et al.* (2002, 2004) considered that the dated lacustrine sediments were buried by the Parinacota debris avalanche deposit, the palaeosoils being incorporated into the avalanche; whereas Francis & Wells (1988) regarded them as post-avalanche lacustrine deposits. The dates from Baied & Wheeler (1993) and Ammann *et al.* (2001) derive from the base of the Laguna Seca lacustrine sequence (in the Cotacotani Lake District area, Fig. 1B), which clearly post-dates the debris avalanche, so, they may provide a more reliable minimum age for the collapse.

The presence of numerous moraines and glacio-fluvial deposits indicate that glaciers extended down to 4450 m a.s.l. during the Pleistocene glaciation (N-II moraines mapped by Ammann *et al.*, 2001). Moraines from the eastern slopes of Ajoya volcano reached the Lauca Basin at 4450 m a.s.l. They are overlain by the Parinacota debris-avalanche deposit and so are older than the collapse (Ammann *et al.*, 2001). Pollen stratigraphy in Laguna Seca (Baied, 1991; Baied & Wheeler, 1993) indicates a gradual transition towards drier and warmer climates starting in the Late Pleistocene and culminating in the mid Holocene dry period. This dry period was followed by a short, wet episode during the late Holocene. One of the most significant changes in the sequence is a transition from carbonate-rich, laminated lacustrine sediments to peat sediments that occurred at about 7030 ± 245 ^{14}C yr BP (Baied & Wheeler, 1993).

The Holocene activity of the Parinacota volcano

Parinacota has been the only active volcano in the Lake Chungará watershed during the Holocene (Wörner *et al.* 1988; de Silva & Francis, 1991). The last eruption was at 290 ± 300 years (Sieber & Simkin, 2002). According to Wörner *et al.* (1988, 2000), the first phase of Holocene activity of the Parinacota volcano (up to 6000 yr BP) emplaced andesite *aa* lava flows that reached the northern edge of the lake where lobate lava morphologies are clearly identified. The second phase of activity (after 6000 yr BP) consisted of a number of eruptions from two small satellite cones (Ajata cones) on the southern flanks. Lavas from these cones are more mafic in composition, and three eruptions have been identified: the *Lower Ajata* lava (6000 yr BP) with abundant clinopyroxene and hornblende, and the *Upper* and *High Ajata* lavas (dated at 3000 and 1400 years ago, respectively) composed of black basaltic andesites with olivine phenocrysts (Wörner *et al.*, 2000). Holocene tephra fallout deposits are scarce: a few layers of fine ash to medium lapilli around Lake Chungará are probably associated with the main vent explosive episodes of Parinacota (Clavero *et al.*, 2004). One major tephra deposit reached 15 km to the east of the volcano and other thin tephra layers are located close to the west flank of the volcano (Clavero *et al.*, 2004). The Lake Chungará succession record, however, contains many tephra layers.

Lake Chungará

Lake Chungará is located at 4520 m a.s.l. in the northern part of the Chungará Subbasin (Fig. 1A), a watershed bounded by high snow-capped volcanoes (Parinacota, Quisquisini, Guallatire, and Ajoya). It has an irregular shape with a maximum length of 8.75 km, maximum depth of 40 m, a surface area of 21.5 km² and a volume of 400×10^6 m³ (Herrera *et al.*, 2006). The western and northern lake margins are steep, formed by the eastern slopes of Ajoya and Parinacota volcanoes. The eastern and southern margins are gentle, formed by the distal fringe of recent alluvial fans and the River Chungará valley.

The morphology of the lake floor has been determined by bathymetric data (Villwock, in Dorador *et al.* 2003) and seismic profiles (Valero-Garcés *et al.*, 2000). Six morphological components can be differentiated along a West-to-East profile (Fig. 2A): (a) a narrow *western littoral platform*, about 175-300 m wide, from 0 to 7 m deep (slope < 1°), (b) a *western slope*, 115 m wide and 7 to 20 m deep, dipping 10°, (c) a 2 to 3° rise at the base of the slope, 115-235 m wide and 25 to 40 m deep, (d) a *central plain*, 4 km wide, from 25 to 40 m deep, (e) an *eastern slope* of 3°, 200 m wide and between 7 and 25 m deep, and (f) a subhorizontal (< 1°) *eastern platform*, 450 to 850 m wide between 0 and 7 m deep. All cores are from sites in the central plain except cores 7, 13 y 14, which are from the rise near the western lake margin, and core 1993, which is from the eastern platform (Fig. 2B).

The climate of the region is semi-arid with annual rainfall between 345 and 394 mm, and an average temperature of 4.2 °C. Evaporation is estimated at 1200 mm/yr (Mladanic *et al.*, 1987). The main inlets to the lake are the Chungará River (300-460 l/s) draining the Guallatire Volcano, and the Ajata and Sopocalane creeks draining the 7 million year old Ajoya stratovolcano (Fig. 1B) (Herrera *et al.*, 2006). The lake has no surface outlet. Underground water discharge from Lake Chungara to the Cotacotani lake system is thought to be about 25 l/s (Herrera *et al.* 2006). Water inputs to the lake (sampled in November 2002) display, on average, the following chemistry: 42 ppm HCO₃⁻, 3 ppm Cl⁻, 17 ppm SO₄²⁻, 7 ppm Na⁺, 4 ppm Mg²⁺, 8 ppm Ca²⁺, 3 ppm K⁺ and 22 ppm Si. The Mg/Ca ratio of water inputs ranges from 0.22 to 0.71, depending on the lithology of the catchment. The lake is polymictic (Muhllhauser *et al.*, 1995) with strong surface currents. Temperature profiles measured in November 2002 showed a gradient from the lake surface (9.1-12.1°C) to the lake bottom (6.2-6.4°C at 35 m of water depth), with a weak thermocline (0.5-0.6°C) at 19 m depth. Oxygen ranged from 11.9-12.5 ppm (surface) to 7.6 ppm (bottom). The pH ranged between 8.99 (surface) and 9.30 (bottom) and the water lake chemistry was: 448 ppm HCO₃⁻, 68 ppm Cl⁻, 354 ppm SO₄²⁻, 140 ppm Na⁺, 99 ppm Mg²⁺, 50 ppm Ca²⁺, 32 ppm K⁺ and 2 ppm Si²⁺. Magnesium and sodium, the most conservative electrolytes, were concentrated in the lake by evaporation, 30 and 20 times respectively. Calcium was concentrated by only 6 times, and dissolved silica was extremely depleted. The phytoplankton community is made up of few species; diatoms and *Chlorophyceae* are dominant during cold and warm seasons, respectively. Macrophyte communities in the littoral zone form dense patches that also contribute to primary productivity. The fauna includes endemic *Cyprinodontid* fish (e.g. 19 species of *Orestias*, Villwock *et al.* 1985). Seasonal measurements of conductivity, nitrate, phosphate and chlorophyll reveal changes in productivity and in the composition of the algal communities related mainly to changes in water temperature and salinity (Dorador *et al.*, 2003). The absence of emerged terraces at the lake margins suggests that the current level of the lake is the highest since the lake formed.

MATERIALS AND METHODS

In November 2002, a coring expedition retrieved 15 cores from Lake Chungará using the raft and the Kullenberg coring equipment of the Limnological Research Center, at the University of Minnesota, USA, where physical properties (GRAPE-density, p-wave velocity and magnetic susceptibility) were measured at 1-cm intervals using a GEOTEK Multi-Sensor Core Logger (MSCL). Cores were split into two, scanned using a DMT colour scanner, and the textures, colours and sedimentary structures were described. About 400 smear slides were prepared for the description of the sediment composition and for semi-quantitative estimates of biogenic, clastic, and authigenic mineral contents using a polarizing microscope. Subsamples were taken every 5 cm for mineralogical, chemical and biological analyses. TIC and TOC contents were sampled every 5 cm and measured by coulometry at Minnesota and at the USGS (Denver).

X-ray fluorescence measurements were conducted with a 2-mm resolution on cores 10 and 11 using the XRF core scanner at the University of Bremen (Germany), using a 60 second count time, 10 kV X-ray voltage and an X-ray current of 1 mA in order to obtain statistically significant data. Samples for x-ray diffraction were dried at 60 °C for 24 hours and manually ground in an agate mill. XRD analysis was done on automatic Siemens D-500 x-ray diffractometer: Cu K α , 40 kV, 30 mA, and graphite monochromator. Initial inspection of the x-ray diffraction patterns revealed a dominant amorphous fraction, characterized by the presence of a broad peak centred between 20° and 25° 2 θ . The identification and quantification of the different mineralogical species present in the crystalline fraction followed a standard procedure (Chung, 1974). The amorphous fraction was quantified by measuring total counts using the XRD software. The sample that showed the highest amorphous peak area (a pure diatomite) was mixed with increasing quantities of pure calcite (5, 10, 20, 40 and 60 wtg %) and the percentage of amorphous content was plotted against total counts. A logarithmic function was adjusted in order to calculate the percentage of the amorphous fraction in all samples. Morphological description and mineralogical identifications were undertaken on representative samples of each facies using a SEM-EDS equipment. Samples were dried in two phases: first, the main amount of water was eliminated by capillarity using filter paper, and then, samples were freeze-dried and vacuum stored prior (and after) carbon coating. Secondary and backscattered electron images and X-ray emission spectra were used systematically to characterize the sediment samples.

Diatom assemblages were quantified every 10 centimetres in core 11 and in a core taken in 1993. Samples were treated following procedures of Renberg (1990). A minimum of 300 valves were counted at x1000 with a Nomarski differential interference contrast microscope Nikon Eclipse E600. Qualitative lake level reconstructions were based on changes in the percentages of diatom life forms (Wolin & Duthie, 1999). As lake level falls, an increase in shallow water habitats induces a proliferation of benthic (bottom dwelling forms) and tychoplanktonic diatoms (those usually having a benthic life form but which can occasionally be facultative planktonic). By contrast, during high lake levels, the percentage of euplanktonic diatoms (those having a strict planktonic character) increases. Pollen sample preparation followed a classic chemical method (Moore *et al.*, 1991; Dupré, 1992), using high-density liquids and adding *Lycopodium* (Stockmarr, 1971) to quantify the pollen concentration. Owing to the low pollen concentration in the sediments, up to 15 g weight samples were taken in core 11 to ensure a sufficient amount of pollen grains. The extreme abundance of *Botryococcus* cysts hindered statistically significant results in many samples.

The chronological model for the Chungará sedimentary sequence is based on 17 AMS ¹⁴C dates (Table 1AB) and 4 U-series disequilibrium dates (Table 1C). The AMS ¹⁴C dates were performed at the Poznan Radiocarbon Laboratory (Poland, Poz samples) and at the Arizona Radiocarbon Facility (Arizona, AA samples). The present-day radiocarbon reservoir effect was determined by radiocarbon dating of the dissolved inorganic carbon (DIC) at Beta Analytic Inc. (Miami). Two litres of lake water were filtered using a polycarbon filter in order to remove all suspended particles, and a small amount of NaOH was added, following the standard protocol of the radiocarbon laboratory. ²³⁴U/²³⁰Th dating was performed at the Minnesota Isotope Lab (MIL) of the University of Minnesota (Table 1C). Four carbonate samples were analyzed by high-resolution ICP-MS using a technique developed at MIL with a Finnigan MAT Element I (Edwards *et al.*, 1987; Cheng *et al.*, 2000; Shen *et al.*, 2002). Up to 17 AMS ¹⁴C dates were obtained from (1) bulk organic matter samples from offshore and (2) aquatic organic macrorests picked from the most marginal cores (Table 1B). The radiocarbon dates were calibrated using CALIB 5.02 software (Reimer *et al.*, 2004). The mid-point of the 95.4 % (2 σ probability interval) was selected for constructing the age model (Table 1B, columns Calibrated age 1 and 2). Seven of the AMS ¹⁴C dates were not used for the chronological model because they showed reversals or non-coherent dates (Table 1B).

RESULTS

Chronology

Dating lacustrine sequences in the Altiplano using ¹⁴C AMS has been hindered by the scarcity of terrestrial macrorests and the large and time-variable reservoir effect (Grosjean *et al.*, 1995, 2001; Geyh *et al.*, 1999; Valero-Garcés *et al.*, 2000). In Lake Chungará, the present-day reservoir effect calculated from the DIC age in lake waters is 2320 \pm 40 ¹⁴C yr BP (Table 1A), close to the values obtained by Geyh *et al.* (1999) from Lake Chungará waters (1754 \pm

160 ^{14}C yr BP) and from living aquatic vegetation (2560 ± 245 ^{14}C yr BP). However, the reservoir effect in the Altiplano lakes has proved to be highly variable in time owing to the interplay of several factors, the lake water volume being the most significant (Geyh and Grosjean, 2000). Accordingly, the correction of the reservoir effect in the Chungará sequence was not performed in the same way in the lower lacustrine (Unit 1) as in the upper lacustrine deposits (Unit 2; see definition of lithostratigraphic units below).

Correction of dates for the variable radiocarbon reservoir effect was based on two assumptions: (1) the present-day lake level is the highest in the lake's history, and (2) the reservoir effect during periods of relatively high lake level (Unit 2) is similar to that one of the present. A constant reservoir effect of 2,320 years (the present-day one) is considered for the upper Unit 2 since the average lake characteristics (depth, water volume) probably did not vary much during the deposition of this unit.

At present, it is only possible to speculate about the variation in time of the reservoir effect in Unit 1. Following Geyh and Grosjean (2000), the reservoir effect was probably lower than in Unit 2 since the lake was, on average, shallower than it was during the deposition of the upper unit. This is supported by (1) the absence of presently emergent former lake terraces, (2) the diatom composition and (3) seismic data (see Results section below). In this work it is proposed to correct the Unit 1 dates for two extreme reservoir age values: a minimum value of 0 years and a maximum of 2,320 years (Table 1B, columns Calibrated age 1 and Calibrated age 2, respectively). A range of age variation for every radiocarbon date of Unit 1 is obtained for these two extreme reservoir effect values. The final chronological model was constructed calculating the mid-point between these two calculated extremes.

Four $^{230}\text{Th}/^{234}\text{U}$ measurements were carried out on calcite crystals that appeared in some thin layers from the Chungará cores (Table 1C). Only one $^{230}\text{Th}/^{234}\text{U}$ date was finally suitable for establishing the chronological model because three samples were rejected due to the high content of ^{232}Th , indicative of high terrigenous inputs.

The uppermost sediments of Lake Chungará were dated by the ^{210}Pb method (Valero-Garcés *et al.*, 2003 and Barra *et al.*, 2004). Very low ^{210}Pb activities at the top of the core (5.41 pCi g^{-1}) posed a significant problem in establishing a reliable chronology. The values of supported ^{210}Pb activity, and the calculated fluxes of unsupported ^{210}Pb were very low (0.18 pCi g^{-1} and 0.20 pCi $\text{cm}^{-2} \text{yr}^{-1}$, respectively), probably a consequence of low atmospheric concentrations of ^{210}Pb in the southern hemisphere and low rainfall on the Altiplano, resulting in a very low atmospheric ^{210}Pb flux. With a stable background activity of 0.18 pCi g^{-1} , the average sedimentation rate in lake Chungará is 0.033 g $\text{cm}^{-2} \text{yr}^{-1}$ or 2.9 mm yr^{-1} (Valero-Garcés *et al.*, 2003), and a similar value (2.4 mm yr^{-1}) was obtained by Barra *et al.* (2004).

Long-term sedimentation rate for the whole sedimentary succession based on AMS ^{14}C and $^{230}\text{Th}/^{234}\text{U}$ dates are considerably lower (0.5 mm/yr core 11 and 0.8 mm/yr core 10, Fig. 3A) than the ^{210}Pb sedimentation rate obtained by Valero-Garcés *et al.* (2003) and Barra *et al.* (2004). The sedimentation rate depends, among other parameters, upon the depositional environments (central plain, rise, littoral zone) and the sedimentary processes involved, and consequently are different for each sedimentary unit (Fig. 3A). Nevertheless, the highest short-term sedimentation rate (2.7 mm/yr) is similar to the modern values, whereas the lowest short-term sedimentation rate is only 0.02 mm/yr (Fig. 3A). Sedimentation rate estimates are lower if volcanoclastic deposits are not considered, particularly in the upper part of the sequence that contains more volcanoclastic layers (Fig. 3B). However, the main sedimentary rate trend remains similar (Fig. 3B): this is discussed below.

Seismic stratigraphy

The cores retrieved in the 2002 expedition allowed a more accurate reinterpretation of the seismic profiles obtained in 1993 with a high-resolution ORE-GEOPULSE (1-12 kHz) system and an EPC 9800 digital graphic recorder (Valero-Garcés *et al.*, 2000). Seismic penetration was not deep, and the presence of gas blanketing, probably due to methane accumulation, obscured the seismic stratigraphy in some profiles. Despite these problems, three seismic units were identified.

Seismic Unit A (profiles SP5 and SP3, Fig. 4A and B). This unit is characterized by the alternation of two seismic facies: i) transparent, and ii) irregular and discontinuous reflectors with cross-cutting relations, and some onlap terminations, suggesting channel morphologies. It has a minimum thickness of 5 m in both the eastern rise and the western part of the central plain.

Seismic features, stratigraphic location and the sedimentological context of the Chungará Basin suggest that this seismic unit corresponds to alluvial-fluvial deposits accumulated prior to the collapse of Parinacota volcano. The deposits are inferred to derive from the Palaeo-Lauca River and they probably extended over the whole central plain.

Seismic Unit B (profiles SP5 and SP3, Fig. 4A and B). This wedge-shaped unit with a minimum thickness of 5 m occurs in the rise of the western margin. It is characterized by the presence of short and mainly convex reflectors with no overall internal structure. The unit grades laterally towards the centre of the basin into the lower part of seismic unit C (SP3), and towards the western margin of the basin, it is overlapped by the upper part of seismic unit C. Core 13

reached sediments of Unit B (basal 15 cm) which consist of massive dark-coloured, coarse gravels and sands, composed of volcanic clasts (up to pebble size). The location, shape and morphology of the internal reflectors are similar to those described by Chapron *et al.* (2004) and Schnellmann *et al.* (2005) and are interpreted as wedges of sublacustrine mass flow deposits that have been deformed by gravity spreading induced by loading of the slope-adjacent lake floor during massflow deposition. The frequent and high-intensity earthquakes in this area of the Central Andes would have favoured these massflow episodes.

Seismic Unit C (profiles SP5, SP3 and SP1, Fig. 4A, B and C). This unit occurs in the rise (cores 3 and 13), the central plain (cores 10 to 12) and in the eastern platform (core 1993). It is made up of transparent seismic facies and parallel horizontal reflectors all over the basin. Its maximum thickness is about 10 m in the north of the central plain and it thins towards both the eastern and western margins. Profiles SP5 and SP3 (Fig. 4A and B) show a discontinuity surface between Units B and C, and the upper 2 m of this unit, overlapping Unit B. This geometry could be interpreted as an indication of a former lower lake level stand followed by a rise in lake level. Several normal faults in profile SP5 affect only the lower part of Unit C, and not the upper sediments. (Fig. 4A). Unit C becomes thicker close to some of the faults, suggesting that the activity of those faults increased the accommodation.

Seismic Unit C corresponds to the lacustrine deposits. Correlation of the seismic profiles with cores shows that the main seismic reflectors correspond to volcanic layers. The thickness and number of these reflectors increase toward the north (eastern margin in profile SP5 and SP3, Fig. 4A and B), suggesting that volcanoclastic deposits come from Parinacota volcano. None of the cores reached the base of the lacustrine sequence in the central plain. The total thickness of the lacustrine sediments in the central plain is estimated to have a minimum of 10 m, the maximum recovery being 8 m in cores 10 and 11.

Sedimentary units, facies and facies associations

Fourteen facies were defined from the cores retrieved in 1993 and 2002 on the basis of detailed sedimentological descriptions, smear slide observations and compositional analyses (Table 2). Most facies are diatomites differentiated by colour and lamination type (Facies A, B, C, D, E) and by the relative abundance of some aquatic macrophyte remains (Facies I, J). Carbonate-rich facies occur in discrete intervals (Facies F, G and H). Alluvial facies are restricted to the lake basin margins (Facies K and L). Volcanoclastic facies (Facies M, N) are particularly abundant in the upper part of the cores. Core log correlation is based on matching the magnetic susceptibility peaks corresponding to tephra layers (M1 to M14, Fig. 5). The fourteen sedimentary facies were grouped into seven lithostratigraphic units corresponding to seven lacustrine and alluvial facies associations on the basis of the stratigraphical correlation (Figs 5A and 5B) and the seismic stratigraphy (Figs 4A, 4B and 4C):

Unit 1. Shallow to deep offshore deposits

Unit 1 deposits correspond to the lower half of seismic unit C (Figs 4A, 4B and 4C). Seismic profiles show that it is thickest in the NW sector of the central plain, and thins to the south (4.07 m in core 11) and west (1 m in core 13), probably overlapping the Miocene substrate. Two subunits were identified in accordance with facies analyses (Figs 5A, 5B, and 6 sections 3 to 6):

Subunit 1a. Finely laminated green diatomite

Subunit 1a reaches at least 2.56 m thick in the south of the central plain (core 11), and thins to the east (0.65 m, core 15) and west (0.58 m, core 13) (Fig. 5A). The deposits are c. 14.1 to 10.2 cal kyr BP in age. The average sedimentation rate was 0.43 mm/yr in core 11 (Fig. 3A).

Facies A dominates Subunit 1a and is composed of diatomite with alternating green and white fine laminae. One 2 cm-thick, glass shard-dominated tephra layer occurs (M1 in cores 11 and 14, Fig. 5B). The diatomite laminations are 0.8 to 10 mm (average 2.9 mm) thick (sections 5 and 6 in Fig. 6). Smear slide and SEM observations show that white laminae are mostly composed of large diatoms. Lamination is defined by changes in the percentage and size of diatom frustules (Fig. 7A), and by variations in the content of amorphous algal organic matter. Diatom frustules show good preservation and no preferred orientation (Fig. 7B) suggesting accumulation from diatomite bloom episodes. The green laminae are composed of smaller diatoms and larger amounts of amorphous algal organic matter than white laminae. Alternating green and white laminae group in 2 to 4 cm-thick bundles in which the white laminae are variously thicker or thinner. Carbonate is absent (Fig. 8) with the exception of disperse fragments of gastropod and bivalve shells. No ostracods are present in these facies. TOC percentages are the lowest (4-8%), increasing towards the top of this unit (Fig. 9).

Euplanktonic diatoms dominate both laminae (average 73%). However, benthic diatoms reach the highest abundance in this facies of all offshore deposits (average 14%). Two intervals rich in benthic diatoms occur towards the base (16-43 %) and top of the unit (11-24 %) and correspond with by the two low percentage peaks of planktonic diatoms in Fig. 9. Pollen concentration is very low in this unit. The presence of the aquatic macrophyte *Myriophyllum* sp. (Fig. 9) suggests relatively shallow water depths, between 0.4 and 4 m, according to data from Lake Titicaca (Ybert,

1992) and Laguna Miscanti (Grosjean *et al.*, 2001). The very low content of *Botryococcus braunii* (Fig. 9) is also another indication for relatively low lake levels given that the development of this algae peaks at water depth greater than 10 m (Carrión, 2002).

Subunit 1a is interpreted as offshore biogenic deposits accumulated in relatively shallow water. Pollen indicators suggest an increase in water depth towards the top of the subunit: *Myriophyllum* is restricted to the base of the subunit whereas the percentages of *Botryococcus braunii* increase towards the top. Diatom assemblages indicate a deepening-shallowing water cycle towards the base of the unit (D1 interval, about c.12.6 kyr cal BP, Fig. 9). The interval rich in benthic diatoms at the top of the unit marks a shallowing-deepening cycle (S1 interval, about c. 10.5 kyr cal BP, Fig. 9). The radiocarbon dates and the number of laminae suggest a pluri-annual frequency, and the occurrence of laminae bundles could be related to multi-decadal cyclicity processes, such as changes in productivity, water temperature and/or lake volume.

Subunit 1b. Laminated and massive brown diatomite and carbonate-rich intervals

Subunit 1b has an age between c. 10.2 and 7.8 cal yr BP, and is composed mainly of two diatomite facies (Facies B and C) and some carbonate-rich intervals at the top. No volcanoclastic layers occur (see K-area curve in Fig. 8, as an indicator of volcanic content due to the presence of potassium in volcanic minerals such as amphiboles and feldspars). The thickness of Subunit 1b varies in the central plain from 1.87 in the north (core 10) to 1.15 in the south (core 11, Fig. 5B). In the rise and the western platform, the thickness thins to 0.73 m in core 15 and 0.62 m in core 13 (Fig. 5A). Sedimentation rate ranges from 0.26 (core 11) to 0.45 mm/yr (core 10, Fig. 3A).

Facies B is a laminated to thin-bedded diatomite (1.1 to 6.0 mm, average 2.6 mm) with brown, white, and some minor reddish laminae. Some intervals show laminae bundles less than 5 cm thick, defined by gradual changes in the thickness of the white laminae (either fining or thickening upwards; Fig. 6, core sections 4 and 5). Brown laminae are commonly fragmented and have a higher percentage of oriented diatoms (Fig. 7C) and contain more amorphous organic matter. The white laminae are almost exclusively composed of diatoms, although some of them also contain carbonate (< 4 %), mostly calcite, with only few intercalated laminae of aragonite. In these carbonate-rich laminae, calcite and aragonite crystals are dispersed in the diatomitic matrix. Calcite crystals are euhedral and about 50 µm long. Aragonite crystals are acicular, about 10 µm long and 2µm wide. Planktonic diatoms account for 88 % of total diatoms and benthic diatoms represent about 9 % on average (Fig. 9). However, an interval from 3.15 to 3.36 m of sediment depth shows higher percentages of benthic diatoms (between 15-31 %) corresponding to the highest carbonate content (4 %, Fig. 9). TOC values are relatively low and resembled those of Facies A (4-8%) (Fig. 9).

Facies C occurs in the upper part of Subunit 1b, in layers 2 to 30 cm-thick, as a massive to banded diatomite, rich in green amorphous organic matter, with fragmented and entire bivalve and gastropod shells. Ostracods are absent. Facies C layers are extensive throughout the basin and were correlated between all cores at the central plain (layers A to C in Fig. 5B). A 30 cm-thick interval located at the top of Unit 1 in core 11 contains two carbonate layers (up to 32 % carbonate) of interbedded Facies C deposits (Fig. 6, section 3). These layers are rich in authigenic calcite and aragonite, similar to those described below as Facies F, with significant percentages of benthic diatoms (5.6 %, Fig. 8).

Although the pollen content is low, *Botryococcus braunii* percentages increase from Subunit 1b to the overlying Unit 2 (from 40% up to 90%, Fig. 9), indicating a rise in lake level. Subunit 1b is interpreted as offshore deposition, relatively deeper than Subunit 1a. However, benthic diatoms and carbonate-rich interval suggest a period of shallower waters (S2 interval, at about 9.8 cal. kyr BP, Fig. 9). The depositional bathymetry of other carbonate-rich intervals is more difficult to interpret (e.g. the top of Subunit 1b, S3 interval, c. 7.8 cal. kyr BP, Fig. 9) because they did not correlate with clear changes in diatomite composition.

Unit 2. Deep (with a shallow event) offshore deposits

This unit corresponds to the upper part of Seismic Unit C (Fig. 4A and B) and occurs in the central plain and the rise. It is composed of massive diatomite with some volcanoclastic layers and carbonates, and it grades laterally to the west and south into alluvial and deltaic deposits, and towards the eastern platform into macrophyte, organic-rich facies (Unit 4, Fig. 5A). Two subunits are identified:

Subunit 2a. Brown massive diatomite with carbonate-rich intervals and volcanoclastics

Subunit 2a has an approximate age between c. 7.8 and 5.7 cal yr BP and its thickness varies greatly from a maximum of 3.44 m in the central plain (core 10), to intermediate values in the central areas (2.18 m in the rise, core 13, 2.29 m in the eastern sector, core 15), and to the lowest values of 1.56 m in the southern areas (core 11). Sedimentation rate of Subunit 2a ranged from 0.94 (core 11) to 2.18 mm/yr (core 10, Fig. 3A). Decrease in thickness of Subunit 2a (compare cores 10, 12, 05 and 11 in Fig. 5B) and the disappearance of some of the lower levels of Subunit 2a (M2, Fig. 5) to the S indicate the existence of onlap close its base. The onlap surface would have developed at c. 7.5 cal kyr BP. The decrease in thickness of Subunit 2A to the west (compare cores 10, 12, 13 and 14, Figs 5A and 5B) is the result of

normal faulting that affects the lower part of seismic unit C (Fig. 4A). Subunit 2a is composed of massive diatomite (Facies D) with intercalated carbonate-rich (Facies E and H) and tephra layers (Facies M and N).

Facies D is brown-red massive and banded diatomite (Fig. 6, sections 3 and 2). Ostracods are particularly abundant in some layers and bivalves and gastropods occur at some levels. Planktonic diatoms commonly represent more than 95 % of the total diatoms (90% in average) (Fig. 9). *Botryococcus braunii* is much more abundant than in Unit 1 (Fig. 9) and TOC values are relatively high (8-11%) (Fig. 9).

Facies F are 1-5 cm-thick, carbonate-rich layers (25 to 55 % carbonate) that occur in a 25 cm-thick, carbonate-rich interval (uppermost 25 cm of section 3, Fig. 6). The carbonate-rich layers form up to 5 % of the thickness of Subunit 2a and are white to pink and made up of calcite, magnesium calcite, aragonite and some traces of dolomite (Fig. 8). Stratigraphic correlation shows that the dominant carbonate mineral in one of the layers changes through the basin. Calcite-rich levels are composed of fibre-bundle crystals (Fig. 7E), fusiform aggregates, rice-shaped crystals and dumbbells (10 to 200 µm long and 6 to 80 µm wide), euhedral crystals (50 to 100 µm in size) and irregular aragonite spheroids (70 to 140 µm in diameter). Ostracodes are abundant in some levels. Aragonite-rich layers show needle-shaped crystals 10 µm long and 1 to 3 µm wide. TOC content varies from 4 to 8 % (Fig. 9). Benthic diatom percentages range between 10 and 21 % and they are more abundant than in Facies D (Fig. 9).

Facies G is a carbonate-breccia in a single layer in core 14, between levels M3 and M4 (Fig. 5B). The breccia is about 40 cm thick, has an erosive contact with the underlying sediments (Fig. 5B), and is composed of angular, cm-thick carbonate clasts within a brown diatomite matrix. Inorganic components of carbonate clasts are similar to those forming carbonate levels of Facies F. The textural features of this breccia suggest a reworked deposit derived from a former, thicker and cemented carbonated level located in more littoral areas.

Volcaniclastic layers in Subunit 2a are Ca-rich andesitic tephra (Ca content 61-247 ppm, Fig. 8), composed of glass, silicate crystals (plagioclases, muscovite, quartz) and pyrite (Fig. 8). Overall, volcaniclastic layers (M2-M7, Fig. 5) account for 20-30 % of the total thickness of Subunit 2a. Two facies can be differentiated:

Facies M are 0.5 to 12 cm-thick massive to graded layers of light grey to greenish grey lapilli; the thickest ones have erosive bases. The lapilli are 0.5-2 cm long, angular, pumice fragments, mostly of glass with minor amounts of quartz and mafic minerals, and have no matrix (layer M5 in section 2, Fig. 6). Most layers grade upwards into fine ash (Facies N). The occurrence of some scouring at the base of the thickest tephra layers suggests current transport. Nevertheless, the uniformity and wide lateral extent of the layers, the common presence of graded bedding, the presence of some aquatic fossils and the scarcity of current-derived features are interpreted as fall-out deposits (e.g. Fisher & Schmincke, 1984). Two cm-thick lapilli layers can be traced throughout the basin (M4 and M5, Fig. 5). The absence of other non-volcanic lacustrine sediments mixed in volcaniclastic layers suggests that there were no significant bottom currents during their deposition.

Facies N is made up of dark grey to black, massive to poorly laminated, 1 to 18 cm thick silty to sandy grain-sized tephra layers, primarily composed of andesine with subordinate amphiboles, glass, quartz and muscovite. Most peaks of magnetic susceptibility and potassium content (measured by the XRF-Scanner) corresponds to these layers (see MS1 and K-areas curves in Fig. 8). Glass shards are a common component of these deposits (Fig. 7D). Most fine tephra layers are cm-thick, display normal grading (see layer M5 in section 2, Fig. 6) and contain diatom fossils. There is no evidence of bottom current reworking. The sedimentological features suggest rapid deposition largely by fall-out. Accumulations of bivalve shells occur at the base of several fine tephra layers. These accumulations are interpreted as *obration* deposits caused by the death of bivalves due to sudden burial under ash (Brett, 1990).

Greater abundance of planktonic diatoms and *Botriococcus* sp. and the absence of *Myriophyllum* sp. of Subunit 2a with respect to Unit 1 suggest relatively deeper conditions in the offshore areas of the lake. However, the peaks in benthic diatoms, corresponding to the carbonate-rich intervals, point to an episode of shallower lake levels (S4 interval, about c. 6.7 cal kyr BP, Fig. 9). Carbonate formation may have been favoured in Subunit 2a by factors such as changes in salinity, stronger diatom blooms, and increases in the input of calcium due to weathering of calcium-rich volcanic material.

Subunit 2b. Dark grey-black, massive diatomite

Subunit 2b ranges from c. 5.7 cal yr BP to present day. Its thickness ranges from 0.86-1.00 m in the central plain, to 1.86 in the platform (core 15) and to 3 m in the rise (core 7; Figs 5A and 5B). The sedimentation rate in the central plain is the lowest recorded in the succession (from 0.09 to 0.34 mm/yr in core 11, Fig. 3A). The Subunit comprises dark grey to black diatomite (Facies E) with abundant volcaniclastic layers (Facies M and N). The volcaniclastic deposits represent between 47 and 56 % of the total thickness of the unit (levels M8-M14, Figs 5A and 5B) and they are andesitic and rhyolitic, with amphibole and a low calcium content (11-52 ppm). A cm-thick rhyolitic white volcaniclastic sand-grade deposit (2.6 cal kyr BP, WAF in Figs 5A and 5B) occurs in all cores and can be correlated with a white volcaniclastic deposit reported in the upper 'Ajata lava flows' (Wörner *et al.*, 1988, 2000).

Facies E have intermediate TOC values (8-10 %) and are progressively darker towards the top due to the increase in mafic minerals dispersed in the diatomitic sediment. Planktonic diatoms dominate the assemblages (95 %, Fig. 9) and benthic diatoms show the lowest percentages of the entire succession. By contrast, *Botryococcus braunii* percentages are the highest in the succession (Fig. 9). No carbonate-rich intervals or benthic diatom peaks were identified, although ostracods are relatively abundant and there are some levels with bivalves and gastropods. This subunit represents deep offshore deposition, about 30-40 m, as the present-day lake water conditions.

Unit 3. Shallow platform deposits

Unit 3 (about c. 7.8 cal kyr BP to Recent) overlies Unit 1 in the central plain. It grades laterally into offshore facies of Unit 2 towards the west, and into the littoral facies of Unit 4 towards the east (Fig. 5A). A sandy interval close to the base of core 15 (Fig. 5A) might correspond with alluvial deposits at the eastern lake margin (Fig. 5A). Unit 3 sediments are the thickest in the eastern areas of the central plain (up to 4.5 m in cores 15 and 9, Fig. 5A), where they are mainly composed of diatomite rich in aquatic macrophyte remains (*Facies I*).

Facies I deposits are made up of massive diatomite with aquatic macrophyte remains, gastropod and bivalve shells. Aquatic plant remains and shells appear dispersed in the diatomite sediment and in discrete, mm- to cm-thick layers. These discrete intervals are more abundant towards the base and the top of the unit, and are similar to *Facies J* (described below), which is dominant in Unit 4. Intercalated tephra layers can be clearly correlated with ones identified in the cores from the central plain. Several calcite- and aragonite-rich intervals correlate with carbonate levels described above as *Facies F* in Subunit 2a.

Two lines of evidence suggest that the depositional environment for Unit 3 was shallower than the one inferred for the laterally equivalent deposits of the central plain: i) the palaeo-relief of the Chungará basin indicates that the eastern area has always been 10-15 m shallower than the western central area, and ii) the abundance of aquatic macrophyte remains. Currently in Lake Chungará, aquatic macrophytes dominate the photic, eastern littoral zone (up to 10-15 m depth) and many macrophyte remains are transported towards the west, suggesting that the most likely source of remains for Unit 3 deposits was the eastern littoral platform (Unit 4).

Unit 4. Shallow to very shallow littoral deposits

Unit 4 (>5 cal yr. BP to Recent) has a minimum thickness of 3.69 m (core 1993) occurring only in the littoral eastern platform, and disappearing towards the slope (Fig. 4C). This unit is made up of non-charophyte-dominated macrophytic peaty deposits (*Facies J*), carbonate-rich, charophyte-dominated deposits (*Facies H*) and some intercalated fine-grained tephra layers (*Facies N*).

Facies J occurs as dm-thick, massive layer composed of variable amounts of cm-long aquatic macrophyte remains (10-25%) in a diatomite matrix. It contains abundant gastropod and bivalve shells. Aquatic plant remains and shells are scattered within the diatomite and concentrated in discrete, mm- to cm- thick layers. TOC values range between 10-17% (Valero-Garcés *et al.*, 2003).

Facies H occurs in cm-thick layers composed of organic matter, diatoms and abundant calcified charophyte remains. Carbonate accounts for 25 % and comprises calcite and minor amounts of Mg-calcite. The most common carbonate components are mineralized intercell areas and calcite-covered charophyte stems (*Chara* sp.). Gastropods, ostracods and bivalves are also abundant (Fig. 7F). Diatoms in Unit 4 from core 1993 contain more benthic diatoms (18-98 %, av. 56) than those from the central plain core (Units 1 and 2). Several discrete levels contain higher planktonic diatom percentages (67 to 82 %).

Facies H and *J* accumulated in the shallow (< 7 m) littoral areas of Lake Chungará, where charophyte and other macrophyte meadows developed, with abundant gastropod and bivalve fauna. The alternation between *Facies H* and *J* indicates a succession of prevelant charophyte meadows and other macrophyte areas, that may relate to changes in water depth and salinity. The eastern littoral platform was only flooded during the final stages of the lake's development. Diatom assemblages also show periods of increased planktonic taxa that could correlate with those identified in the central offshore zones (Unit 2). Carbonate from this unit was clearly bio-mediated by charophyte activity related to the development of *Chara* meadows in littoral zones.

Unit 5. Deltaic and distal alluvial-fan deposits

Alluvial deltaic fine clastic deposits of Unit 5 (*Facies K*) include: (1) deltaic deposits that accumulated on the shallow west platform at the mouths of major creeks draining Ajuya volcano (Fig. 2B), (2) deposits from Chungará River at the southern margin of the lake, and (3) sublacustrine alluvial-deltaic accumulations in the rise in front of the former deltas (interpreted from lake floor morphology, Fig. 2B).

Facies K is composed of dark, well-sorted fine sand and silt.

Shallow deltas developed during the current, high-stand stage of Lake Chungará. Deeper alluvio-deltaic deposits on the slope and rise formed during periods of lake level stability in the previous low-stand stage of Lake Chungará.

Lateral relationships between these alluvial-deltaic deposits with massflow wedge deposits and with lower offshore lake deposits cannot be established.

Distal clastic deposits of a gentle-dip alluvial fan occur in the eastern margin of the lake, and are very similar to the fine clastic sediments of Facies K. The fine sands at the bottom of core 15 (Fig. 5A) could be related to these alluvial fans.

Unit 6. Talus-slope massflow deposits

Wedge-shaped deposits of from sublacustrine massflows on the slope and rise are identified in the western lake by seismic profiles (Unit B, Fig. 4A and B). These deposits (*Facies L*) overlie the Miocene substrate and underlie the laminated deposits of Subunit 1a.

Facies L deposits constitute the lowermost 40 cm of core 13. They are massive, clast-supported gravels (up to pebble size volcanoclasts) in a poorly-sorted, dark sandy matrix. This facies could correspond to pre-lacustrine alluvial material deposited in the basin and reworked by massflow processes.

The sedimentary architecture

The topography of Parinacota volcano prior to its collapse was mainly responsible for the location of the depocentre in the NW of the lake, the lowest point along the Palaeo-Lauca River. The central plain and the rise in the northern sector had the highest accommodation and, consequently, the thickest lacustrine succession (10 m). Eastwards and southwards, the thickness of the lower part of the lacustrine sequence thins out to almost 50 % due lower rates of the sedimentation (Fig. 5). The inherited palaeo-slope of the Palaeo-Lauca River valley suggests that lacustrine deposits probably onlap the Miocene volcanic substrate south and westwards.

A general thickening towards the NW of the central plain affects the lower part of the sedimentary succession (Figs 5A and 5B). Syn-sedimentary normal faulting in the north was responsible for the occurrence of an onlap surface within the lacustrine sequence towards the south and the east (Figs 5A and 5B). The onlap surface corresponds to a sedimentary discontinuity identified by comparing detailed sedimentological logs from cores 10, 11, 12 and 15 (Fig 5). An interval of 40 cm, which includes keylevel M2, is absent in cores 10 and 12 because of this onlap. Subunit 1b, the lower part of Subunit 2a and, probably, Subunit 1a become progressively thinner towards the south and the west (Fig. 5). The uppermost deposits of Subunit 2a and the whole Subunit 2b retain their lateral thicknesses (Figs 5A and 5B), and indicate cessation of normal faulting between the deposition of keylevels M2 and M3 (Subunit 2a).

Lacustrine deposits thin out towards the upper part of the eastern and western tali (Fig. 4A). The thickness of the sediments on the shelves is unknown because seismic penetration was low and there are no long cores from these areas. The eastern platform has at least 3.69 m of sediments (core 1993). In the western platform, streams draining the Ajoja volcano have deposited 20-25 m wide, deltaic sands. Between the delta lobes, the platform is colonized by macrophyte subaqueous vegetation (*Myriophyllum* sp. and others). These modern deltas and sublacustrine deposits suggest lake level stabilized periodically during its overall increase. Absence of a seismic record of the oldest alluvial-deltaic deposits prevents precise correlation with the offshore sediments. Towards the south, the central plain changes abruptly to the slope in front of the delta generated by the Chungará River and the Sopacalane and Chachapay creeks (Fig. 2B). There are no deltaic deposits on the eastern platform since there are no significant streams entering the lake. A large alluvial fan covering the eastern margin of the lake provides only fine-grained material near the lake shoreline. The littoral sediments are fine-grained and the whole platform is covered with macrophytes.

DISCUSSION

The lacustrine record of Parinacota eruptions

The absence of coarse volcanoclastic deposits and deformation structures in Unit 1 lacustrine deposits suggest that Parinacota collapsed prior to the deposition of the oldest sediments recovered from Lake Chungará (between c.12.8 and 15.5 cal kyr BP). These data fit the chronological framework of Wörner *et al.* (2000) who assigned an 18 kyr BP age to the collapse. The abundance of volcanoclastic layers in Unit 2 (upper half of seismic Unit C; Figs 4, 5A, 5B and 8) could indicate that the highest frequency of explosive eruptions occurred between early - mid Holocene (c. 7.8 cal kyr BP) and recent times. Owing to the better preservation in the lake (e.g. Sáez *et al.*, 1999) the number of ash fall deposits in the lacustrine record (about 14) is much higher than that recognized in the subaerial watershed (described by Clavero *et al.*, 2004). The Lake Chungará record demonstrates that volcanic activity - at least explosive activity - was minimal between the Late Pleistocene and early Holocene (from c. 14.1 to 7.8 cal kyr BP). Seismic profiles and stratigraphic correlation show that the thickest volcanoclastic deposits blanketed the entire lake basin (Figs 4 and 5). Changes in reflector amplitude show a general increase towards the northern margin, suggesting that the source of the volcanoclastic material was Parinacota volcano or its satellite cones. Mafic mineral enrichment in volcanoclastic layers from Subunit 2a to Subunit 2b suggests an increasing dominance of mafic-rich eruptions from Ajata satellite cones.

Diatomite deposition in volcanic influenced lakes

The dominance of diatomite in the Lake Chungará offshore deposits is a direct consequence of silica availability. Supply of dissolved silica reflects the hydrolysis of the dominant volcanic minerals in the catchment area (mostly plagioclase, biotite, amphibole and pyroxene minerals). Silica in lake water is extremely depleted compared with inflowing water (see chemical data in previous section) as a result of the uptake by diatoms. Nevertheless, changes in diatomite deposition could also reflect the role of biological processes during the depositional history of the lake, and a simple link between siliceous productivity and volcanic silica availability is not straightforward (Telford *et al.*, 2004). Moreover, the high altitude of Lake Chungará adds some unique features to these biological processes. High-altitude lakes such are mainly characterized by high insolation values and low relative atmospheric moisture. Given that the photic zone reaches lower parts of water column because of the high insolation, benthic algal communities survive at greater depths (>20 m) (Vila & Mühlhauser, 1987). On the other hand, water stratification in high-altitude polymictic lakes occurs for shorter durations. The biota in Lake Chungará must adapt to this high solar radiation and to abrupt temperature changes. This situation gives rise to contrasting periods of strong mixing of the water column and of water stratification. The phytoplankton communities reflect these changes, with *Chlorophyceae* as the dominant group during warm periods and diatoms dominating the cold seasons (Vila & Mühlhauser, 1987; Dorador *et al.*, 2003). The relative abundance of diatom frustules versus *Chlorophyceae* (white versus green laminae respectively) in Unit 1 could respond to temperature controls similar to those at present: warmer periods could be more conducive to *Chlorophyceae* and colder periods would be more favourable to diatoms. Warmer lake waters during relatively lower lake level stages would also be more conducive to *Chlorophyceae* producers (massive, green Facies C) plus gastropod and bivalves. The larger abundance of macrophyte-derived remains within the uppermost sediments of Units 2 and 4 marks an increase in littoral productivity. Extensive flat areas of the Chungará Basin were flooded during the final stages of the rise in the lake level. This is particularly true for the western and eastern platforms, which had slopes less than 1°. These shelf areas were suitable for macrophyte colonization and gave rise to quasi-palustrine conditions before they were completely flooded.

Carbonate formation in volcanically influenced lakes

A variety of mechanisms may trigger carbonate precipitation in lakes (Kelts & Hsü, 1978; Last, 1982). These include a photosynthetic uptake of CO₂ and a consequent increase in carbonate ions by rising pH, an increase of calcium concentration in water, temperature effects on carbonate equilibrium, and the mixing of brines of different compositions. Several processes may work together to cause carbonate precipitation: evaporation of quiet waters may lead to oversaturation of the thin surface layer during the summer months; photosynthetic uptake of CO₂ may increase the pH in the chemocline where the organic productivity is high or in the littoral zone where *Chara* and other aquatic macrophytes proliferate.

Recent waters in Lake Chungará show a non-conservative behaviour of calcium due to its precipitation as carbonate. The chemistry of the water inputs versus the lake water (see Lake Chungará section) also reflects a significant reservoir effect for calcium (and other solutes) in the lake water. Lake Chungará is hydrologically open, with variable water supply (by run-off, rainfall, rivers and groundwater) and outflow (as groundwater and evaporation) and, consequently the water chemistry reflects the net solute balance.

The different carbonate occurrences in Lake Chungará sediments suggest a variety of depositional environments, of which the offshore and littoral environments are the most important. Moreover, calcium availability in the lake waters could have fluctuated over time. The lack of authigenic carbonates in offshore deposits (lowest Subunit 1a) indicates that the calcium content was very low in the earlier stages of lake evolution. Carbonate content increases slowly upwards along the offshore deposits of Subunit 1b, reaching the highest concentration in Subunit 2a. This evolution is consistent with a trend of increasing salinity in Lake Chungará.

Biological factors were crucial for carbonate precipitation, both in the littoral and in the offshore areas. When calcium was not a limiting factor, carbonate production in littoral zones (e.g. core 1993) was related mainly to the respiration-photosynthesis balance of *Chara* and other aquatic macrophytes. Carbonate formation in the eastern margin (reworked carbonate facies of core 14) may have been related to littoral carbonate cementation as there is no clear evidence of subaqueous macrophyte calcification. Carbonate precipitation in the offshore areas was triggered by calcium availability and biological activity (mostly algae). Irregular spacing among carbonate laminae in Subunit 1b suggests that precipitation events were not the result of regular or seasonal temperature fluctuations or regular biota blooms.

Some of the carbonate-rich layers in the offshore sediments of Subunit 2a also occur with calcium-rich (plagioclase-bearing) volcanoclastic layers (see calcium evolution in tephra deposits; Fig. 8). This suggests a link between volcanic eruptions and carbonate production in the lake. Weathering of the calcium-rich volcanic layers in the lake and in the catchment could have caused an increase in the calcium content in the lake water, favouring carbonate precipitation during deposition of Subunit 2a. The increase in water volume during deposition of Subunit 2b (see planktonic versus benthonic diatom evolution Fig. 9) and the decrease in calcium input to the lake could have reduced the offshore precipitation of calcite (see calcium evolution in tephra deposits Fig. 8).

Although calcite (with some magnesium calcite) is the main carbonate in Lake Chungará, aragonite is also present as thin layers offshore. Aragonite laminae occur in many lakes, and aragonite precipitation has been related to fluctuations of the Mg/Ca ratio within lake water (Utrilla *et al.*, 1998; Yu *et al.*, 2002). Precipitation of aragonite laminae in a meromictic saline lake in Canada has been linked to periodic mixing with waters with higher Ca²⁺ concentration, modifying the Mg/Ca ratio (Last & Schweyen, 1985). In Lake Chungará the occurrence of isolated aragonite laminae (Subunit 1b) and aragonite layers (Subunit 2a and Unit 3) that grade laterally into calcite-rich layers may reflect local and small fluctuations of the Mg/Ca ratio in the lake water as a result of differences in Mg/Ca values in the water inputs (see Lake Chungará section).

Controls on the sedimentation rate changes

The sediments of Lake Chungará record significant vertical and lateral changes in sedimentation rate (Fig. 3). Overall, the rate of sedimentation diminished, with a particularly marked decrease in the upper part of Subunit 2a (see arrow *a* in Fig. 3B). The highest short-term sedimentation rate occurred in Subunit 1a (2.25 mm/yr in core 11, Fig. 3A) and the lowest rate occurred in Subunit 2b (0.09 in core 11, Fig. 3A). The main factor that controlled this trend in the central plain of the lake was normal faulting, which affected the lower part of the succession (up to 2 m of vertical displacement). In addition, changes in pyroclastic supply and in the diatom productivity would have influenced the sedimentation rate. The sedimentation rate in the lower part of the succession was enhanced by the accommodation generated by the synsedimentary faulting. Moreover, because photic conditions reach deeper areas at the bottom of the lake, diatom productivity could have been higher during the lowstand period (Unit 1 and Subunit 2a) than during the highstand (Subunit 2b). The maximum sedimentation rates attained in Subunit 2a correlate with (1) the main activity of faults, as determined by faulting and lateral changes in thickness in lower part of Subunit 2a, (2) the deposition of a significant volume of volcanoclastic deposits, and (3) the occurrence of shallow lake level episodes (S3 and S4).

Lateral changes in sedimentation rates can be inferred by comparing sedimentation rate curve of cores 10, 11 and 7 (Fig. 3). The average sedimentation rate in the rise (core 7) is greater than in the central plain (cores 10 and 11), and sedimentation rate values in the northern central plain (core 10) exceed those in the southern central plain (11). The sedimentation rate in the northern central plain was thought to have been higher because of the accommodation generated by the activity of normal faults. The high sedimentation rate in the rise was probably due to the clastic inputs at the foot of the adjacent western slope and due to the high diatom productivity in shallow rise areas.

DEPOSITIONAL HISTORY: TECTONICS, VOLCANIC AND HYDROLOGICAL FORCING

Fluctuations in the level of Lake Chungará during the Late Glacial and the Holocene have been reconstructed using (a) diatom ratios (euplanktonic versus tychoplanktonic plus benthic species), (b) the presence and percentages of littoral macrophytes as *Myriophyllum* sp., (c) percentages of the alga *Botryococcus* sp., (d) variations in sedimentary facies (e.g. Facies C), and (e) the occurrence of carbonate. A progressive increase in lake level in core 11 (central plain) was defined by the increase in euplanktonic diatoms and *Botryococcus* and by the decrease in macrophyte remains (Fig 9). Core 11 did not reach the substrate, so the bathymetry of the early stages of Lake Chungará is unknown. Many lake sequences record shallow basins that became deeper with time (Anadón *et al.*, 1991; Sáez & Cabrera, 2002), but the catastrophic origin of Lake Chungará, due to the impoundment of the river, caused rapid early development of deep depositional environments. This general increase in water volume during the last 15,000 cal yr BP could be attributed to higher water inputs due to enlargement of the watershed. However, there is no geomorphologic evidence of substantial changes in the watershed after the collapse of Parinacota volcano, so the increase in water volume is probably related to changes in the hydrological balance caused by climate change.

The overall increase in lake level is punctuated by a Late Pleistocene deepening episode (D1, Fig. 9) and by at least three shallowing episodes during the lower-mid Holocene (S1, S2 and S4, Fig. 9), identified by the changes in planktonic/benthic diatom ratios. Another shallowing episode (S3?, Fig. 9), in the mid Holocene, is not so well defined, but it also shows an increase in benthic diatoms and is associated with carbonates.

The following stages have been interpreted in the sequence:

Stage 1. Late Pleistocene to onset of Holocene (Fig. 10A)

The Lake Chungará Basin was drained by the Palaeo-Lauca River from N to S prior to the Parinacota debris avalanche. The debris avalanche created an endorheic basin with steep northern and western margins, and the NW part of the basin was almost immediately occupied by a lake. Shortly afterwards, the lake expanded and occupied the entire central plain, and lacustrine facies (Subunit 1a) were deposited on the alluvial sediments of the Lauca River. Maximum water depth was 20 m, as indicated by the absence of sediments of Unit 1a in the eastern lake margin sector. The waters were dilute and calcium-poor. The photic zone reached the lake bed and benthic diatoms and green algae proliferated. Diatoms and green algae dominated sedimentation, and the accumulation rate was high. Green laminae represent periods of stability conducive to diatom and green algae deposition. These periods were interrupted by pluriannual

strong water mixing conditions, which enhanced nutrient availability, triggering exceptional diatom blooms (e.g. Harris, 1996) that deposited to form the white laminae, exclusively made up of diatom skeletons. After the deepening event D1, the dominance of planktonic diatoms suggests that generally deeper conditions prevailed in the lake, punctuated by a shallowing event at about c. 11.7 cal kyr BP. Volcanic activity after the collapse was minor (only one tephra layer) and there was little tectonic activity.

Stage 2. Early Holocene (Fig. 10B)

During the Early Holocene, Subunit 1b sediments were deposited in the central plain. The overall lake-level rise continued reaching a depth of 30 m, although minor lake level fluctuations occurred. The eastern lake margin was progressively flooded, and two fluctuations of shallowing-deepening lake level occurred at c. 9.8 cal kyr BP and at the end of this stage (c. 7.8 cal kyr BP). Sedimentation was mainly biogenic dominated by diatoms and other algal producers. Green and brown laminae represent mixed green algae and diatom sediments; the brown colours could indicate oxidation of the deposits during periods of more oxygenated waters that could correspond to lower lake levels. White laminae represent diatom blooms with pluri-annual periodicity. Conditions for carbonate precipitation occurred during several short intervals. Some of these periods were associated with shallowing lake episodes. No volcanic events were recorded during this period.

Stage 3. Mid Holocene (Fig. 10C)

During stage 3, Subunit 2a was deposited in the central plain. Lake level greatly fluctuated and the western platform was periodically flooded. A shallower lake level episode occurred at c. 6.7 cal kyr BP. Carbonate production peaked in offshore areas during the initial and middle parts of this stage. The flooding of the platforms increased the area of littoral subenvironments in the lake, which were the most carbonate-producing habitats. Increased explosive volcanic activity could also have been conducive to carbonate production due to calcium-rich volcanoclastic inputs, and other changes in water composition. The sedimentation rate was the highest during this period and could be the result of fault activity (increased accommodation), biogenic activity (high TOC) and to carbonate productivity.

Stage 4. Mid-late Holocene to Recent (Fig. 10D)

During stage 4, Subunit 2b sediments were deposited on the central plain. The lake level increased and reached its highest level, although it probably fluctuated around this high stand (30-40 m). The eastern platform was completely flooded and littoral deposition was initiated. Biological productivity in the bottom waters and water-sediment interphase diminished because the photic zone did not reach the lake bottom. Offshore zone carbonate production ceased, possible due to increased dilution with the greater lake volume and smaller calcium inputs. Sedimentation rates decreased as a result of lower biological activity. Carbonate productivity continued in the littoral zone (core 1993) and there is evidence of carbonate deposition in the northern margin of the central plain (20 m water depth) during the last 500 years (Valero-Garcés *et al.*, 2003).

CONCLUSIONS

1. Lake Chungará was formed by the collapse of Parinacota volcano prior to 12.8 cal. kyr BP. Seismic profiles and core stratigraphy show alluvial-fluvial deposits beneath the 10 m-thick, lacustrine succession of Lake Chungará. The age of the oldest dated lake sediments (between c. 12.8 to 15.5 cal kyr BP) is consistent with the chronological framework assigning an 18 kyr BP age to the Parinacota collapse (Wörner *et al.*, 2000).

2. The sedimentary architecture of the Holocene lacustrine succession was controlled by a) the inherited palaeo-relief and b) changes in the accommodation caused by lake level fluctuations and tectonic subsidence. The first factor determined the location of the depocentre in the NW sector of the central plain. The second factor caused the expansion of lacustrine deposition towards the eastern and southern margins, and the accumulation of sediments on the elevated marginal platforms.

3. A period of normal fault activity occurred during the deposition of Unit 1 and the lower part of Unit 2. The deposits were affected by normal faults with displacements of a few meters in the northern sector of the basin. The faulting increased the accommodation and the sedimentation rate in the northern depocentre, and generated an onlap surface within the lacustrine succession.

4. Diatoms were the main producers in Lake Chungará. This reflects the availability of silica in the volcanic setting. Increases in benthic diatom productivity during lowstand periods led to parallel increases in the sediment rate. The relatively high TOC values (8-11 %) suggest that other algae such as *Botriococcus* sp. could also have played a significant role in the depositional history of the lake. The biogenic productivity in littoral zones was dominated by charophytes (*Chara* sp.) and other macrophytes (*Myriophyllum* sp.). Green and brown laminae reflect periods of deposition characterized by the dominance of diatom and other alga producers whereas white laminae indicate diatom blooms.

5. Well preserved volcanoclastic sedimentary records in Lake Chungará have allowed a reconstruction of the local eruptive history after the collapse of Parinacota volcano. Some lava flows occurred in the early Holocene, but explosive eruptions were rare during the Late Pleistocene and early Holocene (c. >12.8 to 7.8 cal kyr BP). From mid Holocene (c. 7.8 cal kyr BP) to the present, explosive activity from Ajata satellite cones increased. The first phase of this eruptive period was mafic-poor and calcium-rich (Subunit 2a). After c. 5.7 cal kyr BP, the composition of the volcanoclastic materials became mafic-rich and calcium-poor (Subunit 2b).

6. Carbonate in volcanic-influenced lakes has different origins to lakes in non-volcanic settings. Littoral productivity associated with Charophytes peaked when suitable shallow shelves were available for colonization. Offshore carbonate precipitation in Lake Chungará peaked during mid Holocene, approximately at c. 7.8 and 6.4 cal kyr BP. Two main factors favoured the carbonate formation: (a) the rise in lake water salinity due to evaporation, and (b) increased input of calcium due to emplacement of volcanoclastic material from Parinacota volcano into the lake and into the broader catchment.

7. Changes in the aquatic flora (diatoms and aquatic macrophytes) and the presence of carbonate layers reflect the lake level fluctuations: a) a deepening episode at Late Pleistocene (about c. 12.6 cal kyr BP), b) four shallowing episodes at early-mid Holocene (about c. 10.5, 9.8, 7.8 and 6.7 cal kyr BP), c) higher lake levels at late-mid Holocene (since c. 5 cal kyr till present). Laminated diatomite from Unit 1 shows a pluri-annual to decadal frequency of biogenic deposition.

ACKNOWLEDGEMENTS

The Spanish Ministry of Science and Education funded the research at Lake Chungará through the projects ANDESTER (BTE2001-3225), BTE2001-5257-E and LAVOLTER (CGL2004-00683/BTE). The Limnological Research Center (U of MN, USA) provided the technology and expertise to retrieve the cores, and the facilities for the Initial Core Descriptions. We are very grateful to CONAF (National Forestry Authority of Chile), the Dirección General de Aguas de Chile (Water Authority) and to the staff at the Lauca National Park. The Palaeostudies programme (European Science Foundation) provided the funding necessary to carry out the analysis at the University of Bremen by A. Moreno in December 2003. We wish to thank Walter Dean (USGS, Denver) for help with elemental carbon analyses. We are particularly indebted to D. Schnurrenberger, A. Myrbo and M. Shapley (LRC, USA) ensuring the success of coring expedition to the lake. Thanks to G. Wörner for suggestions on volcanics. P. Anadón, C. Beck, and M. Branney are acknowledged for suggestions to improve and clarify the earlier version.

REFERENCES

- Anadón, P., Cabrera, L., Julià, R. and Marzo, M. (1991) Sequential arrangement and asymmetrical fill in the Miocene Rubielos de Mora Basin (Northeast Spain). In: *Lacustrine facies analysis*. (Eds P. Anadón, L. Cabrera-L., K. Kelts). *Spec. Pub. Int. Assoc. Sediment.*, **13**, 257-275.
- Amman, C., Jenny, B., Kammer, K. and Messerli, B. (2001) Late Quaternary Glacier response to humidity changes in the arid Andes of Chile (18-29°S). *Palaeogeogr., Palaeoclimatol., Palaeoecol.*, **172**, 313-326.
- Baied, C.A. (1991) *Late-Quaternary environment, climate and human occupation of the South-Central Andes*. Ph.D. Dissertation, University of Colorado, Boulder, 131 pp.
- Baied, C.A. and Wheeler, J.C. (1993) Evolution of High Andean Puna ecosystem environment, climate and culture change over the last 12,000 years in the Central Andes. *Mountain Research and Development*, **13**, 145-156.
- Baker, P., Williamson, D., Gasse, F. and Gibert, E. (2003) Climatic and volcanic forcing revealed in a 50,000 year diatom record from Lake Massoko, Tanzania. *Quater. Res.*, **60**, 368-376.
- Bao, R., Sáez, A., Servant-Vildary, S. and Cabrera, L. (1999) Lake-level and salinity reconstruction from diatom analyses in Quillagua Formation (Late Neogene, Central Andean Forearc, Northern Chile). *Palaeogeogr., Palaeoclimatol., Palaeoecol.*, **153**, 309-335.
- Barra, R., Pozo, K., Muñoz, P., Salamanca, M.A., Araneda, A., Urrutia, R. and Forcadi, S. (2004) PCBs in a dated sediment core of a high altitude lake in the Chilean Altiplano: The Chungará Lake. *Fresenius Environmental Bull.* **13**, 83-88.
- Bellanca, A., Calvo, J.P., Censi, P., Elizaga, E. and Neri, R. (1989) Evolution of lacustrine diatomite carbonate cycles of miocene age, southeastern Spain - Petrology and isotope geochemistry. *J. Sedimen. Petr.*, **59**, 45-52.
- Brett, C.E. (1990) Ostracod deposits. In: *Palaeobiology. A synthesis*. (Eds. D.E.G. Briggs and P.R. Crowther). Blackwell Scientific Publications, Oxford, 239-243.

- Carrión, J.S.** (2002) Patterns and processes of Late Quaternary environmental change in a montane region of southwestern Europe. *Quatern. Sc. Rev.*, **21**, 2047-2066.
- Cheng, H., Edwards, R.L., Hoff, J., Gallup, C.D., Richards, D.A. and Asmeron, Y.** (2000) The half-lives of uranium-234 and thorium-230. *Chemical Geol.*, **169**, 17-33.
- Chung, F.H.** (1974) Quantitative interpretation of X-Ray diffraction patterns of mixtures. *J. Appl. Cryst.* **7**, 519-531.
- Clavero, J.E., Sparks, S.J. and Huppert, H.E.** (2002) Geological constraints on the emplacement mechanism of the Parinacota debris avalanche, northern Chile. *Bull. Volcanol.*, **64**, 40-54.
- Clavero, J.E., Sparks, S.J., Polanco, E. and Pringle, M.** (2004) Evolution of Parinacota Volcano, Central Andes, Northern Chile. *Rev. Geol. Chile*, **31**, 317-347.
- Colman, S.M., Kelts, K.R. and Dinter, D.A.** (2002) Depositional history and neotectonics in Great Salt Lake, Utah, from high-resolution seismic stratigraphy. *Sed. Geol.*, **12**, 61-78.
- Chapron, E., Van Rensbergen, P., De Batist, M., Beck, C. and Henriot, J.P.** (2004) Fluid-escape features as a precursor of a large sublacustrine sediments slide in Lake Le Bourget, NW. Alps, France. *Terra Nova*, **16**, 305-311.
- de Silva, S. and Francis, P.** (1991) *Volcanoes of the Central Andes*. Springer-Verlag, 216 p. Berlin.
- Dorador, C., Pardo, R. and Vila, I.** (2003) Temporal variations of physical, chemical and biological parameters of a high altitude lake: the case of Chungará Lake. *Rev. Chilena de Hist. Nat.*, **76**, 15-22.
- Dupré, M.** (1992) *Palinología*. Soc. Española de Geomorfología. 30 pp.
- Edwards, R.L., Chen, J.H. and Wasserburg, G.J.** (1987) ^{238}U - ^{234}U - ^{230}Th - ^{232}Th systematics and the precise measurement of time over the past 500,000 years. *Earth and Planet. Sci. Lett.*, **81**, 175-192.
- Fisher, R.V. and Schmincke, H.U.** (1984) *Pyroclastic rocks*. Springer-Verlag. Berlin. 472 pp.
- Francis, P.W. and Wells, G.** (1988) Landsat thematic mapper observations of debris avalanche deposits in the Central Andes. *Bull. Volcanol.*, **50**, 258-278.
- Gasse, F., Fontes, J.C., Plaziat, J.C., Carbonel, P., Kaczmarzka, I., Deckker, P.D., Soulié-Marsche, I., Callot, Y. and Dupeuble, P.A.** (1987) Biological remains, geochemistry and stable isotopes for the reconstruction of environmental and hydrological changes in the holocene lakes from North Sahara. *Palaeogeogr., Palaeoclimatol., Palaeoecol.*, **60**, 1-46.
- Gaupp, R., Kött, A. and Wörner, G.** (1999) Palaeoclimatic implications of Mio-Pliocene sedimentation in the high-altitude intra-arc Lauca Basin of northern Chile. In: *Ancient and recent lacustrine systems in convergent margins* (Eds L. Cabrera and A.Sáez). *Palaeogeogr., Palaeoclimatol., Palaeoecol.*, **151**, 79-100.
- Geyh, M.A. and Grosjean, M.** (2000) Establishing a reliable chronology of lake level changes in the Chilean Altiplano: a result of close collaboration between geochronologists and geomorphologists. *Zbl. Geol. Paläont. Teil I*, **7/8**, 985-995.
- Geyh, M.A., Grosjean, M., Nuñez, L. and Schotterer, U.** (1999) Radiocarbon reservoir effect and the timing of the late-glacial/early Holocene humid phase in the Atacama Desert (Northern Chile). *Quater. Res.*, **52**, 143-153.
- Grosjean, M.** (1994). Paleohydrology of the Laguna Lejía (north Chilean Altiplano) and climatic implications for late-glacial times. *Paleogeogr., Paleoclimatol., Paleoecol.*, **109**, 89-100.
- Grosjean, M., Geyh, M.A., Messerli, B. and Schotter, U.** (1995) Late-glacial and early Holocene lake sediments, groundwater formation and climate in the Atacama Altiplano. *J. Paleolimnol.*, **14**, 214-252.
- Grosjean, M., Valero-Garcés, B.L., Geyh, M.A., Messerli, B., Schreier, H. and Kelts, K.** (1997) Mid and Late Holocene Limnogeology of Laguna del Negro Francisco, northern Chile, and its paleoclimatic implications. *The Holocene*, **7**, 151-159.
- Grosjean, M., van Leeuwen, J.F., van der Knaap, W., Geyh, M., Ammann, B., Tañer, W., Messerli, B., Núñez, L., Valero-Garcés, B. and Veit, H.** (2001) A 22,000 ^{14}C yr B.P. sediment and pollen record of climate change from Laguna Miscanti (23° S), northern Chile. *Global Planet. Change*, **28**, 35-51.
- Haberle, S.G., Szeicz, J.M. and Bennett, K.D.** (2000) Late Holocene vegetation dynamics and lake geochemistry at Laguna Miranda, XI Region, Chile. *Revista Chilena de Historia Natural*, **73**, 655-669.
- Harris, G.P.** (1986). *Phytoplankton Ecology*. Chapman and Hall, London. 384 pp.

- Herrera, C., Pueyo, J.J., Sáez, A. and Valero-Garcés, B.L.** (2006) Relación de aguas superficiales y subterráneas en el área del Lago Chungará y lagunas de Cotacotani, norte de Chile: un estudio isotópico. *Rev. Geol. Chile*, **33**, 299-325.
- Kelts, K. and Hsü, K.** (1978) Freshwater carbonate sedimentation. In: *Lakes-Chemistry, Geology, Physics* (Ed A. Lerman), Springer, New York, pp. 295-323.
- Kött, A., Gaupp, R. and Wörner, G.** (1995) Miocene to Recent history of the western Altiplano in northern Chile revealed by lacustrine sediments of the Lauca Basin (18 degrees 15'-18 degrees 40'S/ 69 degrees 30'-69 degrees 05'W). *Geol. Rundsch.*, **84**, 770-780.
- Last, W.M.** (1982) Holocene carbonate sedimentation in Lake Manitoba, Canada. *Sedimentology*, **29**, 691-704.
- Last, W.M. and Schweyen, T.H.** (1985) Late Holocene history of Waldsea Lake, Saskatchewan, Canada. *Quater. Res.*, **24**, 219-234.
- Mladinic, P., Hrepic, N. and Quintana, E.** (1987) Water physical and chemical characterization of the lakes Chungará and Cotacotani. *Archivos de biología y medicina experimentales*, **20**, 89-94.
- Moore, P., Webb, J.A. and Collinson, A.** (1991) *An illustrated guide to pollen analysis*. London. Hodder and Stroughton. 216 pp.
- Muhlhauser, H., Hrepic, N., Mladinic, P., Montecino, V. and Cabrera, S.** (1995) Water-quality and limnological features of a high-altitude andean lake, Chungará in northern Chile. *Rev. Chilena de Hist. Nat.*, **68**, 341-349.
- Owen, R.B. and Crossley, R.** 1992. Spatial and temporal distribution of diatoms in sediments of Lake Malawi, Central Africa, and ecological implications. *J. Paleolimnol.*, **7**, 55-71.
- Owen, R.B. and Utha-aroon, C.** (1999) Diatomaceous sedimentation in the Tertiary Lampang Basin, Northern Thailand. *J. Paleolimnol.*, **22**, 81-95.
- Reimer, P.J., Baillie, M.G.L., Bard, E., Bayliss, A., Beck, J. W., Bertrand, C.J.H., Blackwell, P.G., Buck, C.E., Burr, G.S., Cutler, K.B., Damon, P.E., Edwards, R.L., Fairbanks, R.G., Friedrich, M., Guilderson, T.P., Hogg, A.G., Hughen, K.A., Kromer, B., McCormac, G., Manning, S., Ramsey, C.B., Reimer, R.W., Remmele, S., Southon, J. R., Stuiver, M., Talamo, S., Taylor, F.W., van der Plicht, J. and Weyhenmeyer, C.E.** (2004) IntCal04 Terrestrial Radiocarbon Age Calibration, 0-26 Cal Kyr BP. *Radiocarbon*, **46**, 1029-1058.
- Renberg, I.** (1990) A procedure for preparing large sets of diatom slides from sediment cores. *J. Paleolimnol.*, **4**, 87-90.
- Sáez, A. and Cabrera, L.** (2002) Sedimentological and palaeohydrological responses to tectonics and climate in a small, closed, lacustrine system: Oligocene As Pontes Basin (Spain). *Sedimentology*, **49**, 1073-1094.
- Sáez, A., Cabrera, L., Jensen, A. and Chong, G.** (1999) Late Neogene lacustrine record and paleogeography in the Quillagua-Llamara basin, Central Andean fore-arc (Northern Chile). In: *Ancient and Recent Lacustrine Systems in Convergent Margins* (Eds L. Cabrera and A. Sáez). *Palaeogeo., Palaeoclim., Palaeoec.*, **151**, 5-37.
- Schnellmann, M., Anselmetti, F.S., Giardini, G. and McKenzie, J.A.** (2005) Mass movement-induced fold-and-thrust belt structures in unconsolidated sediments in Lake Lucerne (Switzerland). *Sedimentology*, **52**, 271-289.
- Shen, C.C., Edwards, R.L., Cheng, H., Dorale, J.A., Thomas, R.B., Moran, S.B. and Edmonds, H.N.** (2002) Uranium and thorium isotopic and concentration measurements by magnetic sector inductively coupled plasma mass spectrometry. *Chem. Geol.*, **185**, 165-178.
- Sieber, L. and Simkin, T.** (2002) *Volcanoes of the World: an Illustrated Catalog of Holocene Volcanoes on their Eruptions*. Smithsonian Institution. Global Volcanism Program Digital Information Series, GVP-3. URL: <http://www.volcano.si.edu/world/>.
- Stockmarr, J.** (1971) Tablets with spores used in absolute pollen analysis. *Pollen Spores*, **13**, 614-621.
- Telford, R.J., Barker, P., Metcalfe, S. and Newton, A.** (2004) Lacustrine responses to tephra deposition: examples from Mexico. *Quater. Sci. Rev.*, **23**, 2337-2353.
- Utrilla, R., Vazquez, A. and Anadón, P.** (1998) Paleohydrology of the Upper Miocene Bicorn Lake (easter Spain) as inferred from stable isotopic data from inorganic carbonates. *Sedim. Geol.*, **121**, 191-206.
- Valero-Garcés, B.L., Delgado-Huertas, A., Navas, A. and Ratto, N.** (1999a) Large ¹³C enrichment in primary carbonates from Andean Altiplano lakes, Northwest Argentina. *Earth Planet. Sci. Lett.*, **17**, 253-266.
- Valero-Garcés, B.L., Grosjean, M.; Schreier, H.; Kelts, K. and Messerli, B.** (1999b) Holocene lacustrine deposition in the Atacama Altiplano: facies models, climate and tectonic forcing. *Palaeogeogr., Palaeoclimatol., Palaeoecol.*, **151**, 101-125.

- Valero-Garcés, B.L., Grosjean, M., Messerli, B., Schwalb, A. and Kelts, K.** (2000) Late Quaternary Lacustrine Deposition in the Chilean Altiplano (18°-28° S). In: *Lake basins through space and time*. (Eds E.H.Gierlowski-Kordesch and K. Kelts). *AAPG Studies in Geol.*, **46**, 625-639.
- Valero-Garcés, B.L., Delgado-Huertas, A., Navas, A., Edwards, L., Schwalb, A. and Ratto, N.** (2003) Patterns of regional hydrological variability in central-southern Altiplano (18°-26°S) lakes during the last 500 years. *Palaeogeogr., Palaeoclimatol., Palaeoecol.*, **194**, 319-338.
- Vila, I. and Mülhauser, H.** (1987) Dinámica de lagos de altura, perspectivas de investigación. *Archivos de Biología y Medicina Experimentales* (Chile), **20**, 95-103.
- Villwock, W., Kies, L., Thiedig, F. and Thomann, R.** (1985) Geologisch-ökologische Untersuchungen am Lago Chungará / Nord Chile: Zielsetzungen und erste Ergebnisse. *IDESIA (Chile)*, **9**, 21-34.
- Wolin, J.A. and Duthie, H.C.** (1999) Diatoms as indicators of water level change in freshwater lakes. In: *The Diatoms: Applications for the Environmental and Earth Sciences* (Eds E.F. Stoermer and J.P. Smol), pp. 183-202. Cambridge University Press, Cambridge.
- Wörner, G., Harmon, R.S., Davidson, J., Moorbath, S., Turner, D.L., McMillan, N., Nye, C., López-Escobar, L. and Moreno, H.** (1988) The Nevados de Payachata volcanic region (18°S/69°W, N. Chile). I. Geological, geochemical, and isotopic observations. *Bull. Volcanol.*, **50**, 287-303.
- Wörner, G., Hammerschmidt, K., Henjes-Huns, F., Lezaun, J. and Wilke, H.** (2000) Geochronology ($^{40}\text{Ar}/^{39}\text{Ar}$, K-Ar and He-exposure ages) of Cenozoic magmatic rocks from Northern Chile (18°-22° S): implications for magmatism and tectonic evolution of the central Andes. *Rev. Geol. Chile*, **27**, 205-240.
- Ybert, J.P.** (1992) Ancient lake environments as deduced from pollen analysis. In: *Lake Titicaca A synthesis of limnological knowledge* (Eds C. Dejoux and A. Iltis). Kluwer Academic Publishing, Dordrecht, pp. 49-60.
- Yu, Z.C. Ito, E. and Engstrom, D.R.** (2002) Water isotopic and hydrochemical evolution of a lake chain in the northern Great Plains and its paleoclimate implications. *J. Paleolimnol.*, **28**, 207-217.
- Zheng, Z. and Lei, Z.Q.** (1999) A 400,000 year record of vegetational and climatic changes from a volcanic basin, Leizhou Peninsula, southern China. *Palaeogeogr., Palaeoclimatol., Palaeoecol.*, **145**, 339-362.

FIGURE CAPTIONS

Figure 1. A map of the Lauca Basin and the two subbasins that were created by the collapse of Parinacota volcano: the Chungará and the Cotacotani subbasins. Lake Chungará occupies the highest subbasin. It is topographically closed and surrounded by >5500 m a.s.l. volcanoes (modified from Kött *et al.*, 1995). B. Geological map of the Lake Chungará area.

Figure 2. A; A bathymetric map of Lake Chungará showing the main morphological units of the lake floor. B. Map of Lake Chungará depicting littoral alluvial deposits, the main syn-sedimentary faults, the location of the 1993 and 2002 cores and the 1993 seismic profiles.

Figure 3. Inferred sedimentation rate curves for the Chungará succession showing short-term values. Curves for the northern (core 10) and southern (core 11) sectors of the central plain and the rise (core 7) are represented. The model was constructed using 8 AMS ^{14}C and 1 $^{230}\text{Th}/^{234}\text{U}$ radiometric dates, and correlation between cores. The AMS ^{14}C dates of Subunit 2b were corrected using the present-day reservoir effect value (2320 yr), whereas dates for Subunits 1a and 1b were corrected using mean values between 2320 yr and 0 yr. The date point for Subunit 2a corresponds to the $^{230}\text{Th}/^{234}\text{U}$. A. Sedimentation rate curves including volcanoclastic deposits. B. Sedimentation rate curves without the volcanoclastic deposits. Arrow (a) indicates the main trend of increasing sedimentation rate (see text for further explanation).

Figure 4. A. Seismic profile SP5, a cross-section perpendicular to the western margin of the lake. B. Seismic profile SP3, a cross section parallel to the western margin of the lake. C. Seismic profile SP1, a cross-section perpendicular to the eastern lake margin. Locations of the seismic profiles are indicated on figure 2B. TWTT: two way trend time scale.

Figure 5. A. West-East stratigraphic cross-section. B. North-South stratigraphic cross-section. Stratigraphic correlations are based on lithostratigraphic and sedimentological criteria (limits between units and some key levels and facies) and magnetic susceptibility profiles. In cross-section A, note that there is no lateral continuity with Unit 4 (core 1993) in the eastern platform. To improve clarity, the horizontal scales are not the same in the central trough as in the platforms.

Figure 6. Image of Core 11 taken with a DMT scanner (LRC, Minnesota). Facies, lithological units and ^{14}C AMS radiocarbon dates and main magnetic susceptibility peaks (M1 to M11 and WAF) are indicated. Black arrows indicate radiocarbon dates in core 11 and are expressed in *c. yrs cal BP* (Table 1).

Figure 7. SEM microphotographs of the diatomite, volcanoclastic and carbonate facies. A. *Facies A*, white-green diatomite laminites. Lamination is marked by diatom content and size; in this case note the sharp change from small to large diatoms (Subunit 1a, core 11, section 6, cm 22). B. *Facies A*. Detail of the upper part of previous photograph. The good preservation of diatoms together with the absence of a preferred orientation of frustules suggests accumulation from a diatomite bloom episode. C. *Facies B*, white-brown diatomite laminites (Subunit 1b, core 11, section 3, cm 14), the high fragmentation and orientation of diatoms suggest some clastic reworking of this deposit. D. *Facies N*. Detail of fine-grained tephra (Subunit 2a, core 11, section 3, cm 40); note in the centre, a vesicular glass grain. E. *Facies F*. Detail of calcite crystals in a carbonate layer. Crystals are composed of fibre-bundles (Subunit 2a, core 11, section 3, cm 5). F. *Facies H*. Littoral carbonate-rich sediments with abundant Charophyte (*Chara* sp) and ostracode remains. Observe the mineralized intercell areas and calcite-covered charophyte stems (Unit 4, core 1993).

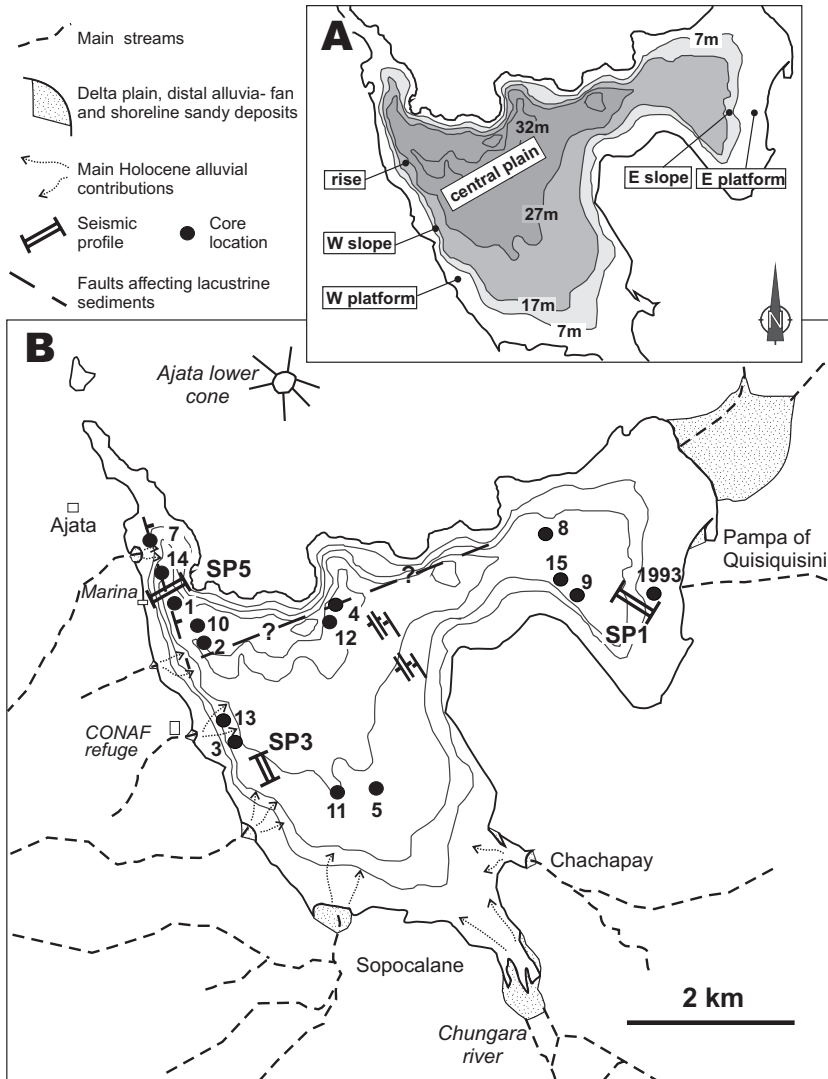
Figure 8. Magnetic susceptibility, potassium curve and calcium content in tephras (K-area) from a composite log of cores 10 and 11. CaCO_3 % curve and mineralogy curves are from core 11 (Fig. 2). The magnetic susceptibility and potassium curves mark the presence of tephra layers in the lacustrine succession. Calcium content in the volcanoclastics and mineralogy curves show mainly changes in tephra composition. Calcium content in tephras show calcium-rich volcanic inputs in Subunit 2a. CaCO_3 % curve shows a maximum presence of offshore carbonates in the same interval.

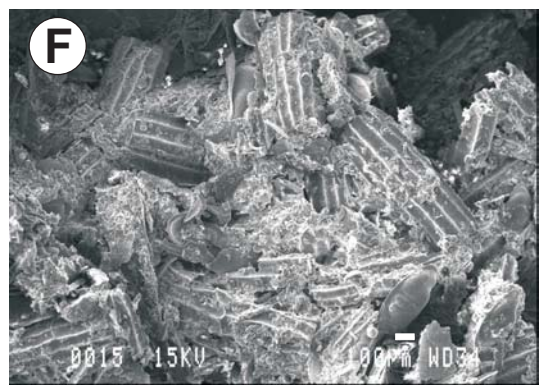
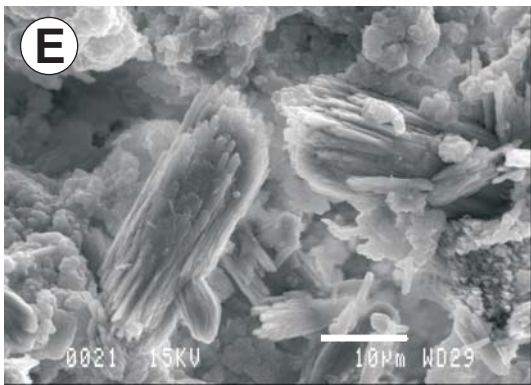
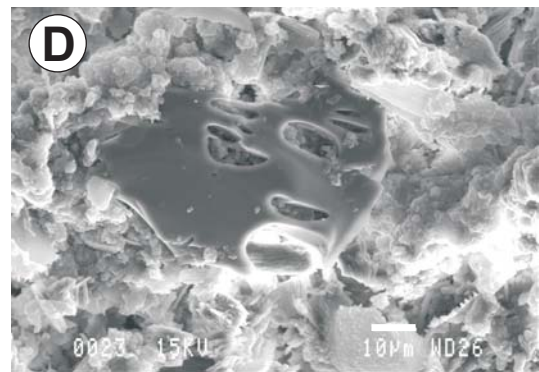
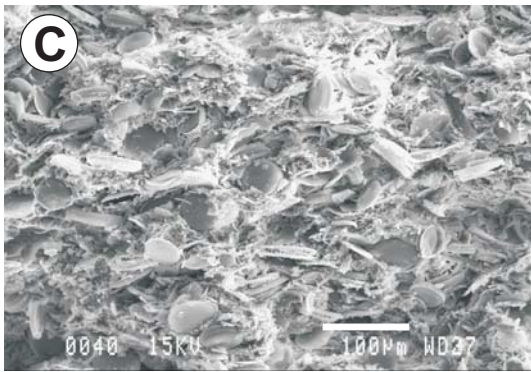
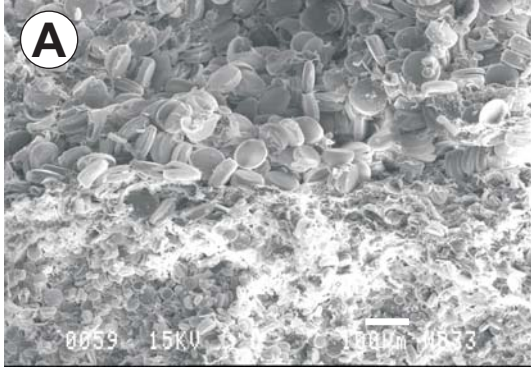
Figure 9. Biological indicators (TOC %, *Botryococcus* and planktonic diatom percent abundances of the total palynomorph and diatom assemblages respectively) and CaCO_3 % profiles from core 11 (Fig. 2). The lake level evolution curve, based on these proxies, is shown on the right side. Deepening-shallowing episode (D1) and shallowing-deepening episodes (S1, S2, S3 and S4) are indicated. The lake deepened overall. *Botryococcus* content is expressed as a percentage of the total particles observed in the pollen slides, including pollen, microcharcoal particles, cysts and unknown plant remains. The percentage of planktonic diatoms versus the addition of tycolanktonic and benthonic diatoms is shown.

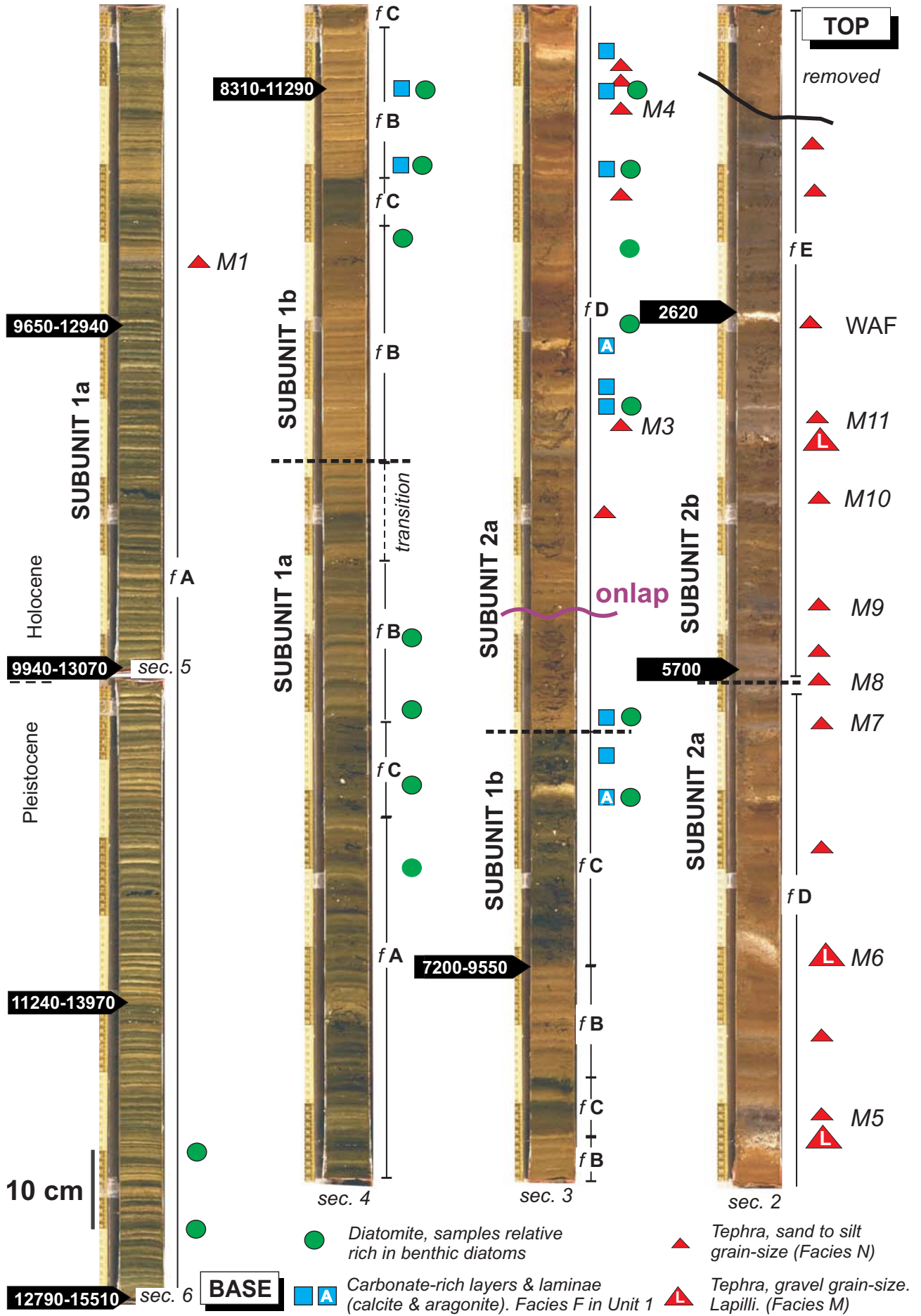
Figure 10 Evolution of Lake Chungará in the last 14,000 years. From stage 1 to stage 4, the lake expanded and deepened. Active faulting affected lake sediments during stages 2 and 3. The main volcanic activity occurred during stages 3 and 4. Calcium-rich volcanoclastic deposits are recognized only in stage 3. Main aquatic macrophyte production was mostly located in the eastern margin of the lake.

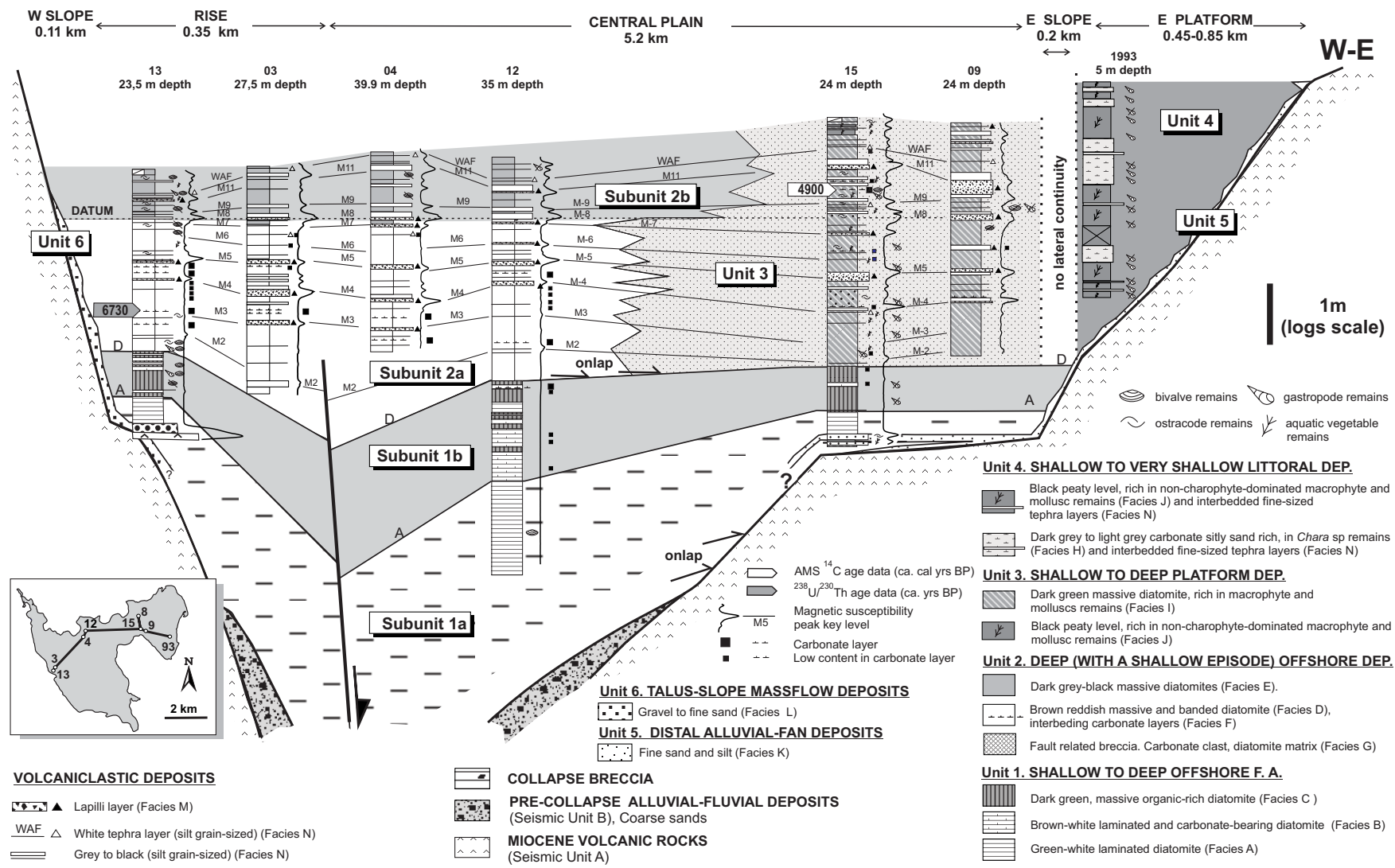
Table 1. A. AMS ^{14}C radiocarbon age of the present-day DIC in Lake Chungará surface water (sampled in 2003). B. ^{14}C AMS radiocarbon age measured in bulk organic matter and aquatic organic macroremains of Lake Chungará core samples. C. $^{230}\text{Th}/^{234}\text{U}$ ages measured in carbonate crystals of Lake Chungará core samples. Shaded and (*) samples are not included in the final chronological model (reversal dates or high values of ^{232}Th). See text for calibration procedures.

Table 2. Facies and facies associations in Lake Chungará sediments.

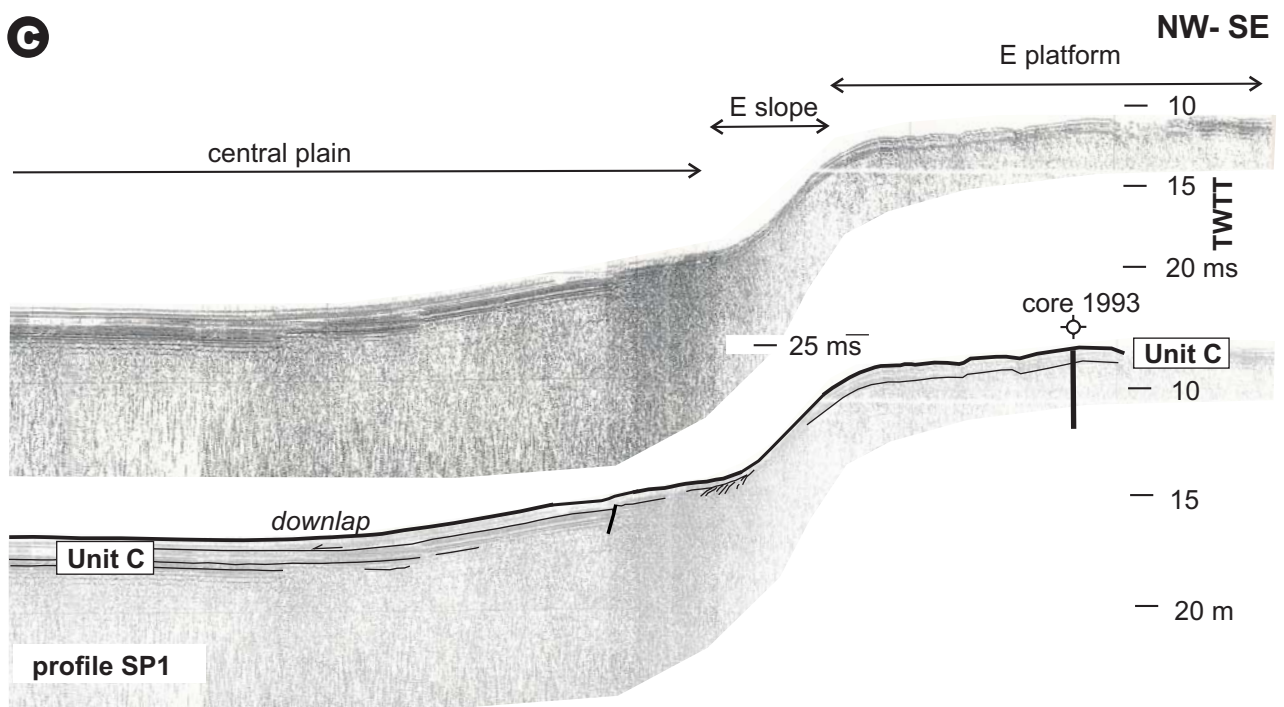


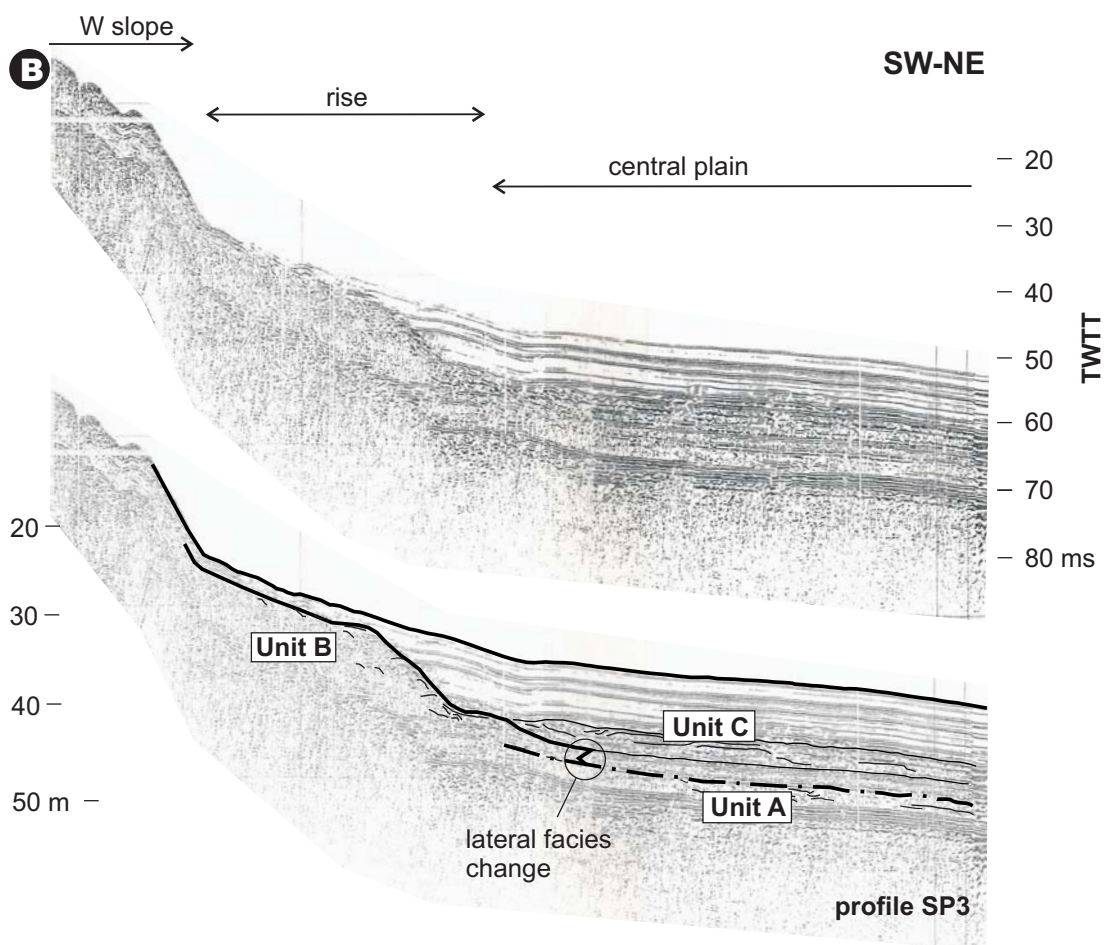
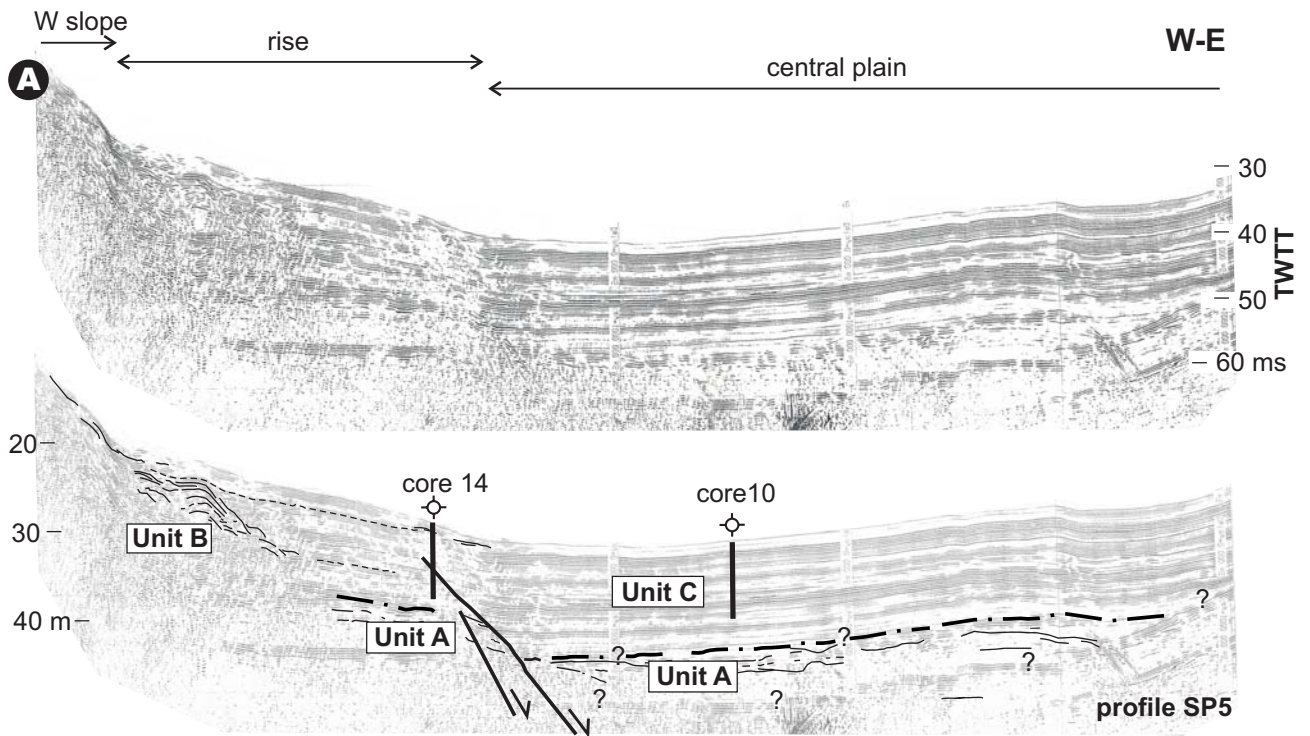


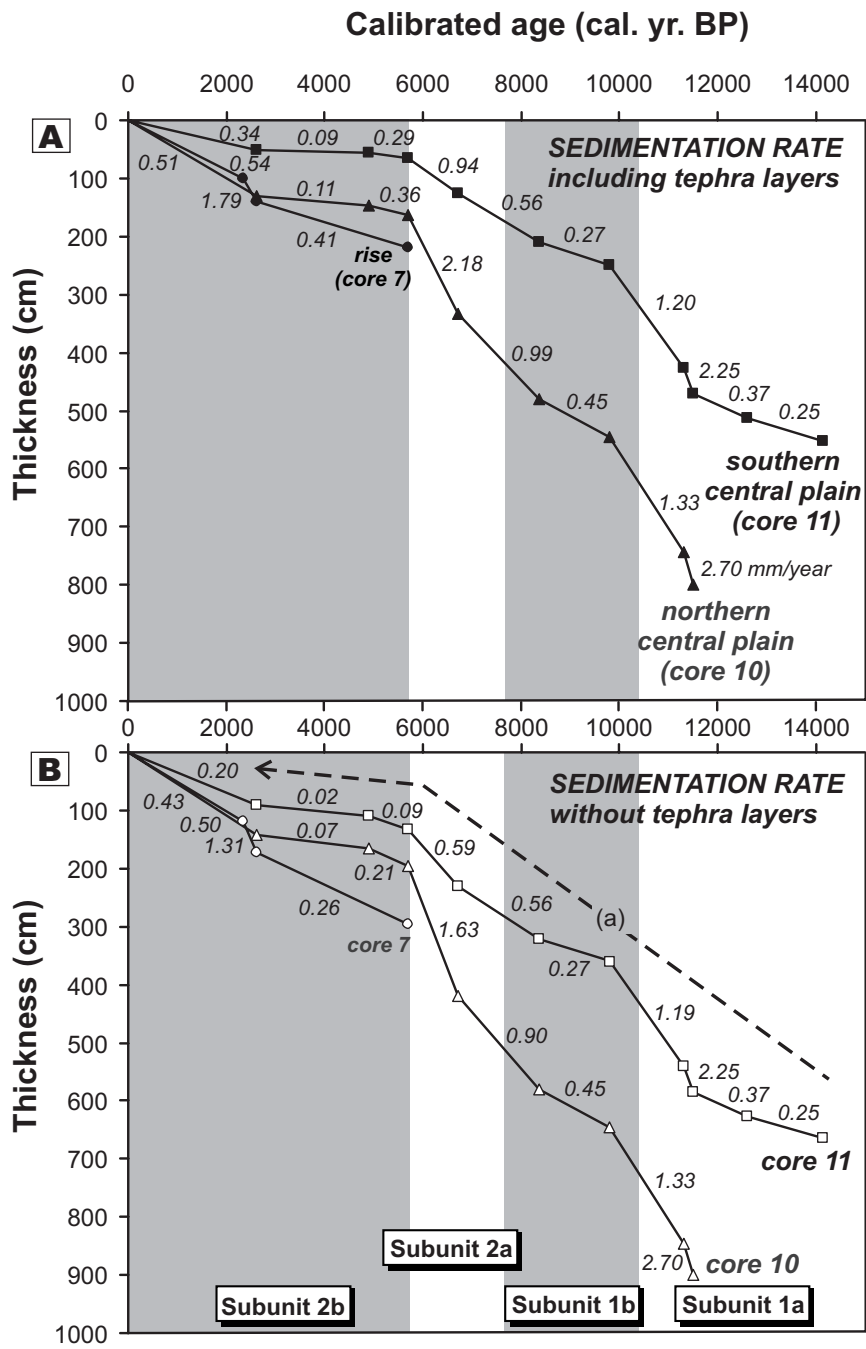


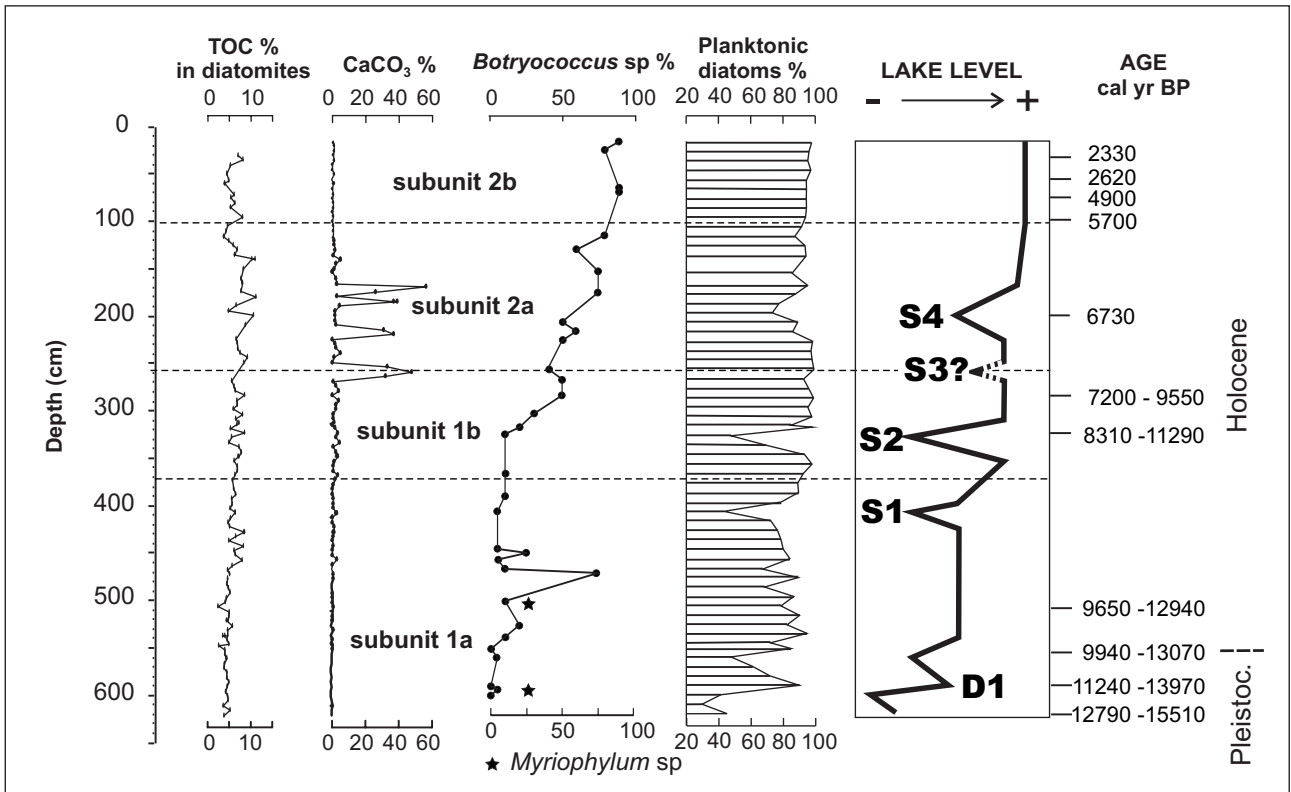


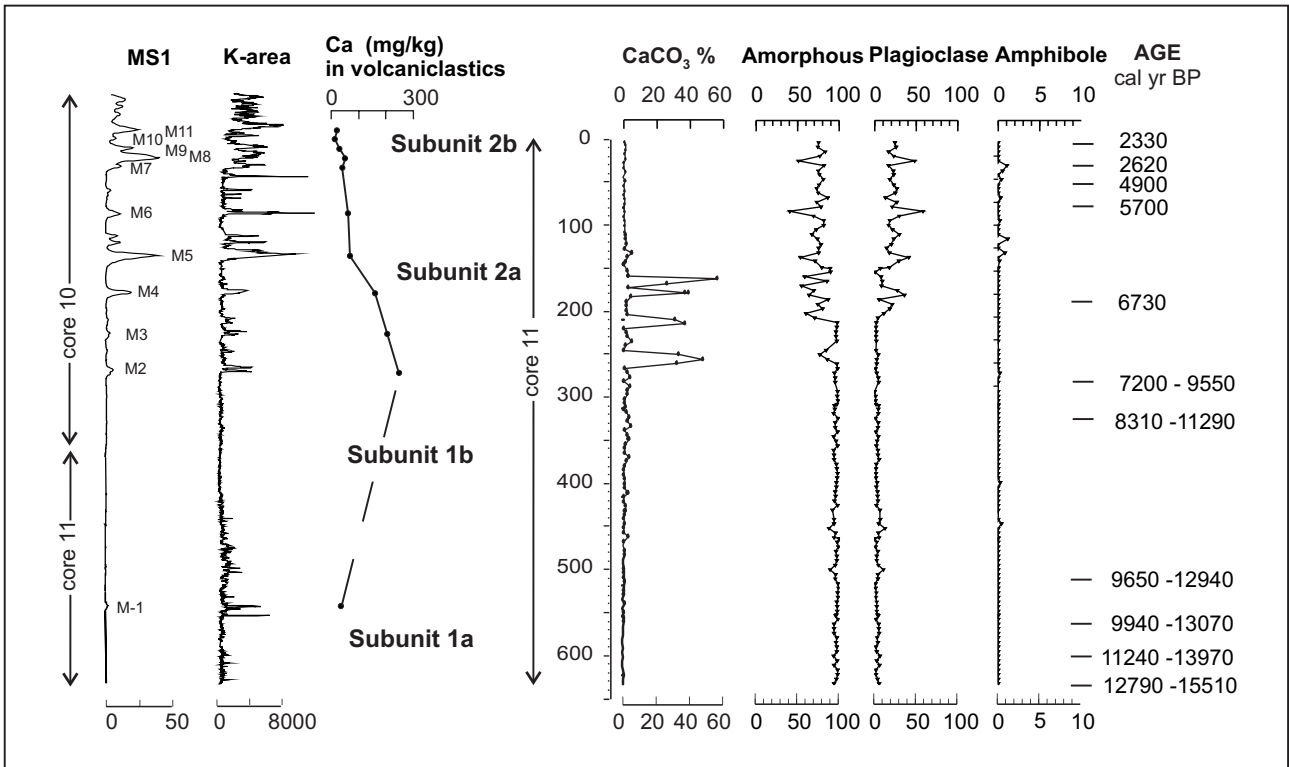
C

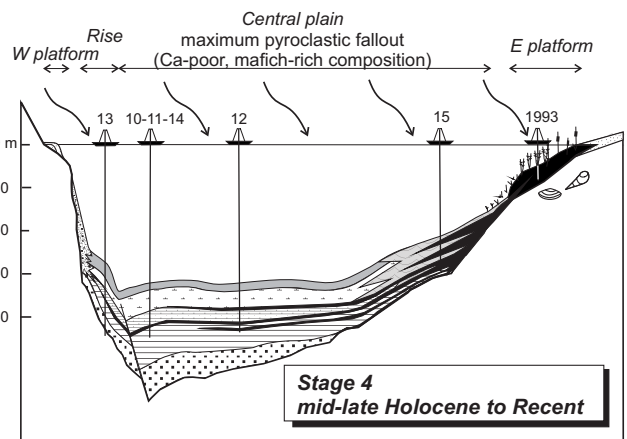
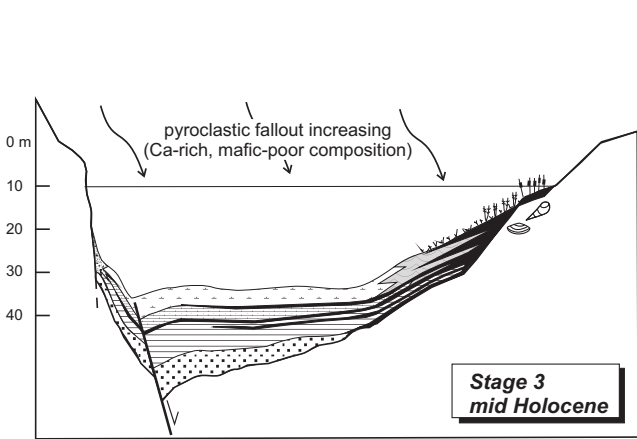
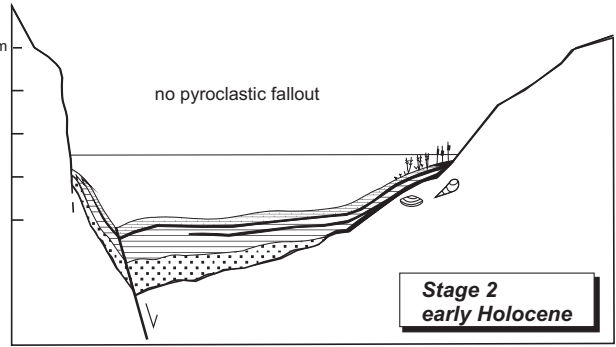
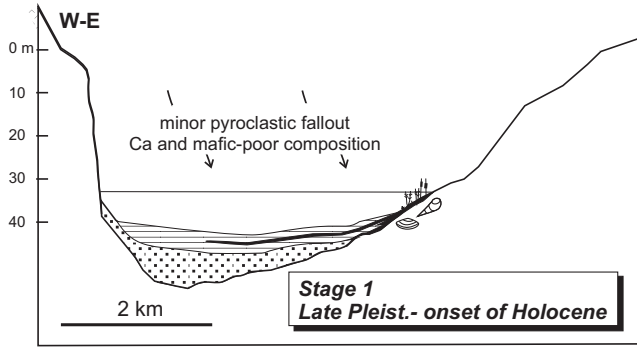




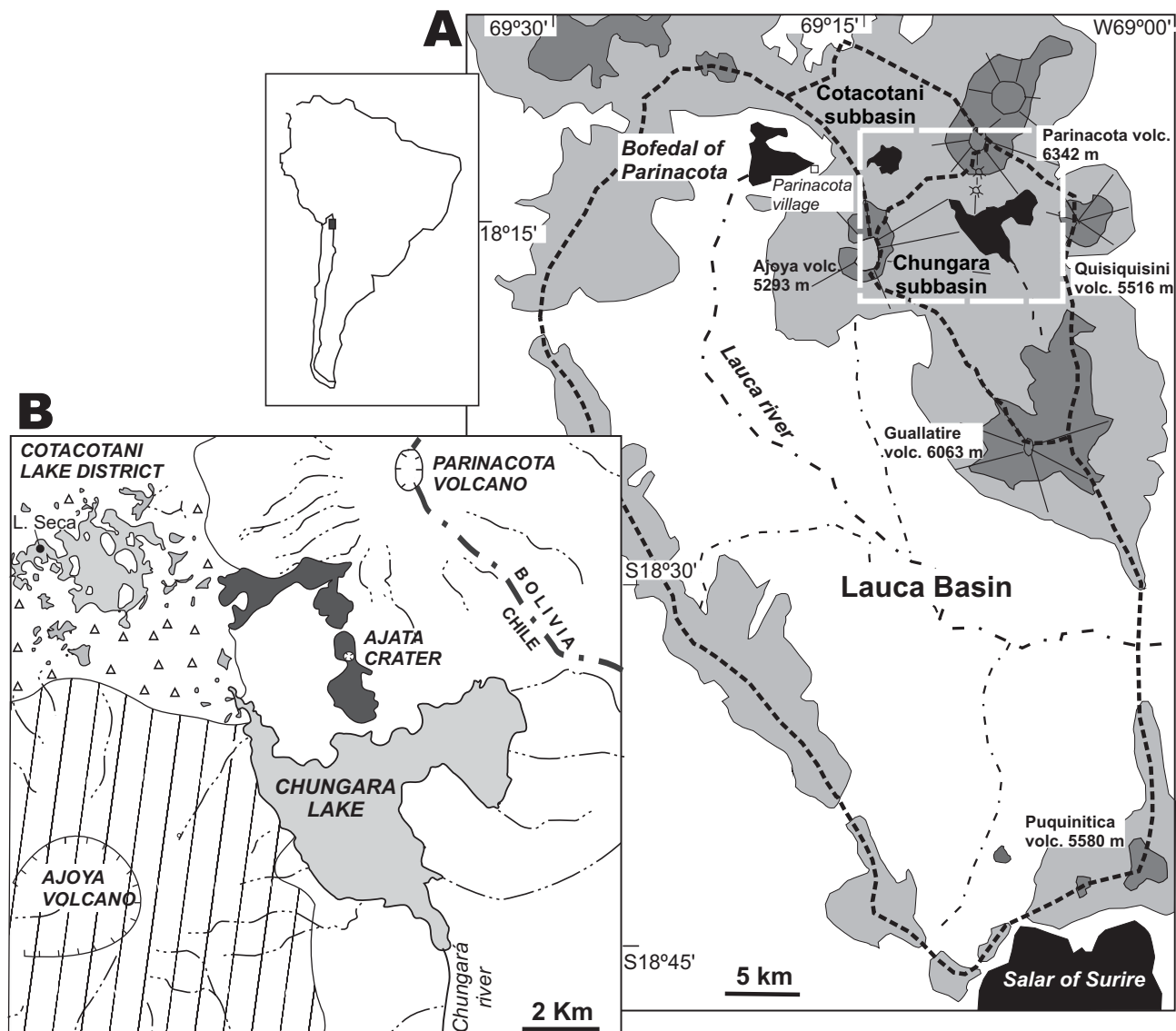








- | | | | |
|---|---|---|---|
| bivalves | gastropodes | SUBUNIT 2a. Diatomite, carbonate and tephra layers | UNIT 4. Peat, silt and diatomite |
| charophytes and other aquatic macrophytes | SUBUNIT 1b. Carbonate laminated diatomite | UNIT 3. Aquatic macrophyte and mollusc-rich diatomite | UNIT 6. Gravel, sand and silt (deformed masflows) |
| PRE-COLLAPSE, FLUVIAL-ALLUVIAL DEPOSITS | SUBUNIT 1a. Laminated diatomite | SUBUNIT 2b. Mafic minerals-rich diatomite and tephra layers | UNIT 5. Fine sand and silt |



- Ajata Holocene lavas
- Parinacota debris avalanche deposit
- Pleistocene-holocene volcanic rocks
- Miocene volcanic rocks

- ALTITUDE**
- < 4500 m
 - 4500-5000 m
 - > 5000 m
- volcano
 - lakes, playa-lakes (salar) and swampy areas (bofedal)
 - Hydrological catchment area